NAVAL POSTGRADUATE SCHOOL
Monterey, California

THESIS

ANALYSIS OF INCOMPRESSIBLE CASCADE FLOWS USING "STATE-OF-THE-ART" COMPUTER PROGRAMS

by

Paul E. Genskow

March 1985

Thesis Advisor: M. F. PLATZER

Approved for Public Release; Distribution is Unlimited

SECURITY CLASSIFICATION OF THIS PAGE *(When Data Entered)*

REPORT DOCUMENTATION PAGE

READ INSTRUCTIONS BEFORE COMPLETING FORM

1. REPORT NUMBER	2. GOVT ACCESSION NO. / 3. RECIPIENT'S CATALOG NUMBER
4. TITLE *(and Subtitle)*: Analysis of Incompressible Cascade Flows using "State-of-the-Art" Computer Programs	5. TYPE OF REPORT & PERIOD COVERED: Master's Thesis, March 1985
	6. PERFORMING ORG. REPORT NUMBER
7. AUTHOR(s): Paul E. Genskow	8. CONTRACT OR GRANT NUMBER(s)
9. PERFORMING ORGANIZATION NAME AND ADDRESS: Naval Postgraduate School, Monterey, California 93943	10. PROGRAM ELEMENT, PROJECT, TASK AREA & WORK UNIT NUMBERS
11. CONTROLLING OFFICE NAME AND ADDRESS: Naval Postgraduate School, Monterey, California 93943	12. REPORT DATE: March 1985
	13. NUMBER OF PAGES: 64
14. MONITORING AGENCY NAME & ADDRESS *(if different from Controlling Office)*	15. SECURITY CLASS. *(of this report)*: UNCLASSIFIED
	15a. DECLASSIFICATION/DOWNGRADING SCHEDULE

16. DISTRIBUTION STATEMENT *(of this Report)*

Approved for Public Release, Distribution Unlimited

17. DISTRIBUTION STATEMENT *(of the abstract entered in Block 20, if different from Report)*

18. SUPPLEMENTARY NOTES

19. KEY WORDS *(Continue on reverse side if necessary and identify by block number)*

Incompressible Cascade Flows, Computer Programs Analysis

20. ABSTRACT *(Continue on reverse side if necessary and identify by block number)*

Two "state-of-the-art" computer programs, Q3DFLOW and a standard Cebeci boundary layer program as applied to aerodynamic flows in a cascade are examined. Q3DFLOW is a quasi three-dimensional finite element turbomachinery program. Only the incompressible blade-to-blade module of this program is used. The Cebeci boundary layer program is for incompressible, two dimensional, and constant viscosity flows. It is used to calculate

DD FORM 1 JAN 73 1473 EDITION OF 1 NOV 65 IS OBSOLETE

S/N 0102-LF-014-6601

SECURITY CLASSIFICATION OF THIS PAGE *(When Data Entered)*

boundary layers on a few isolated airfoils and airfoils/blades in a cascade. Experimental data and other analytical computations are compared for both programs. Additionally, the theory and operation of the Cebeci boundary layer program are presented.

Approved for public release; distribution is unlimited.

Analysis of Incompressible Cascade Flows using "State-of-the-Art" Computer Programs

by

Paul E. Genskow
Captain, United States Marine Corps
B.S., Iowa State University, 1977

Submitted in partial fulfillment of the
requirements for the degree of

MASTER OF SCIENCE IN AERONAUTICAL ENGINEERING

from the

NAVAL POSTGRADUATE SCHOOL
March 1985

ABSTRACT

Two "state-of-the-art" computer programs, Q3DFLOW and a standard Cebeci boundary layer program as applied to aerodynamic flows in a cascade are examined. Q3DFLOW is a quasi three-dimensional finite element turbomachinery program. Only the incompressible blade-to-blade module of this program is used. The Cebeci boundary layer program is for incompressible, two dimensional, and constant viscosity flows. It is used to calculate boundary layers on a few isolated airfoils and airfoils/blades in a cascade. Experimental data and other analytical computations are compared for both programs. Additionally, the theory and operation of the Cebeci boundary layer program are presented.

TABLE OF CONTENTS

LIST OF TABLES

LIST OF FIGURES

TABLE OF SYMBOLS

s	space between blades in cascades
c	chord length
μ	viscosity
ν	kinematic viscosity
ρ	density
p	local static pressure
u	velocity component in x direction (i.e. tangential to surface)
v	velocity component in y direction (i.e. normal to surface)
α	angle of attack, i.e. angle between oncoming flow and the chord
β	angle between flow direction and horizontal axis of cascade
γ	stagger angle
σ	solidity, s/c
$-\rho\overline{u'v'}$	Reynolds shear stress
ε_m	"two-range" eddy viscosity

ACKNOWLEDGEMENTS

First and foremost , I acknowledge God, my creator and his only begotten Son, Jesus Christ, my Lord and Savior through whom all things are made possible. I am grateful to my wife, Kelly and my two daughters, Sarah and Ruth with whom God has blessed me. I thank Professor Platzer and Professor Moses for stimulating my interest in the field of cascade aerodynamics and all other professors and students at the Naval Postgraduate School that I had contact with for making the learning experience worthwhile. I would also like to thank Dr. Cebeci and Dr. Hirsch for the use of their programs and assistance.

1. INTRODUCTION/BACKGROUND

Two important parameters of interest in the field of aerodynamics of airfoils are lift and drag. Lift is defined as the force generated by an airfoil normal to the mean free stream direction of flow. Lift can be approximated by integrating the pressure distribution around an airfoil. Drag is the component of force parallel to the mean free stream direction of flow. Drag on airfoils is usually defined to consist of two forms, skin friction drag and pressure drag where the total drag on the airfoil is usually defined as profile drag. Drag on airfoils is more difficult to calculate and predict than lift.

Flow separation occurs when the fluid "particles" fail to follow the surface of the airfoil. Separation is sometimes confused with the phenomenon of stall. Stall can not occur without separation but separation can occur without stall. Separation is usually a three dimensional effect and incorporating this effect into lift and drag calculations on airfoils which are two dimensional is a very difficult task. Prediction of drag on airfoils on a purely theoretical basis is difficult even when the flow has not separated since transition of the flow from laminar to turbulent significantly affects the drag.

Laminar flow is distinguished from turbulent flow visually by the macroscopic motion of the fluid. Laminar flow appears smooth to the eye while turbulent motion is very erratic to the eye. The physical mechanisms that induce this motion are different. Generally speaking, most flows of interest start laminar (steady) and transition to turbulent (unsteady). The start and finish point of transition is very difficult to predict. This transition point or range is usually empirically determined.

The unsteady nonlinear three dimensional Navier Stokes equations define the macroscopic motion of a Newtonian fluid. A Newtonian fluid is a fluid in which the stresses are related to the rates of strain of the fluid particle and the coefficient of viscosity. Air is assumed to be

governed by these equations. However, until recently there was no practical method of solution to these equations. Due to this difficulty the Navier Stokes equations were reduced to two general sets of equations:

1. Inviscid/potential
2. Viscous/boundary layer.

The inviscid equations are further simplified by assuming steady flow, no external body forces,and no energy transfer to or from the fluid. With the additional assumption of uniform approach flow the flow is irrotational and hence permits the introduction of a velocity potential. The inviscid/potential flow solution is of limited value because it predicts no viscous drag (D'Alembert's paradox). However,in combination with the Kutta-Joukowski condition the inviscid solution predicts the lift of airfoils with sharp trailing edges at small angles of attacks very well. The condition originally proposed by Kutta in 1902 and independently by Joukowski in 1906 [Ref. 1: pp. 390-395] asserts only that the upper and lower surface flows meet smoothly at the trailing edge. This condition is sometimes referred to as a zero load condition at the trailing edge, meaning there is a pressure equalization at the trailing edge.

The Kutta condition is a practical solution to the problem that the inviscid flow solution is singular when the flow negotiates a sharp corner (that is the velocity goes to infinity) for an arbitrary circulation. Placement of a rear stagnation point eliminates this problem and introduces a unique solution to the inviscid equations. Experimental evidence supports the theory of circulation and the Kutta condition on airfoils with relatively sharp trailing edges at small angles of attack. However, in certain flow regimes the inviscid/potential flow solution with the Kutta condition fails to adequately explain real world flow phenomena, such as flows around wings at high angles of attack and practical turbomachinery blades in cascades. Here the effects of viscosity can no longer be ignored.

With the effects of viscosity included, the unsteady Navier Stokes equations are difficult to solve. Simplification is accomplished by

discarding higher order terms. These simplified Navier Stokes equations are now termed boundary layer equations. The boundary layer concept , first introduced by Prandtl in 1904, defines a very thin region next to the surface of an object where all significant velocity gradients normal to the streamwise direction occur and hence viscous forces are generated. Outside this region all viscous forces are assumed negligible and the inviscid/potential solution is assumed to adequately model the flow. The boundary layer equations can predict the drag on airfoils since most drag is due to skin friction caused by the viscous forces in attached flow. The problem is made more difficult by the need to compute both laminar and turbulent boundary layers and to determine the transition point from laminar and turbulent flow. The reader is also reminded that the boundary layer concept is applicable only at sufficiently high Reynolds numbers. For a more detailed discussion of the boundary layer concept see Schlichting [Ref. 2] and Cebeci and Bradshaw [Ref. 3].

Turbulent flows are difficult to predict and model. Alleviation of the unsteady nature of turbulent flows is generally accomplished by expressing the pertinent variables of the unsteady three dimensional Navier Stokes equations as a time averaged quantity and a fluctuating quantity and then time averaging the equations term by term. These time averaged Navier Stokes equations produce nine additional unknown entities that can be correlated to a stress tensor. These extra turbulent unknowns are termed Reynolds stresses. However, all nine Reynolds stresses are not considered significant. In fact, only one Reynolds stress is usually retained in a two dimensional analysis, which is the case for the Cebeci program used in this thesis. This Reynolds stress is the shear stress that is in the normal plane to the surface in the streamwise direction. It is considered the turbulent counterpart to the laminar shear stress. This particular Reynolds stress is sometimes modeled as the product of an empirical "eddy viscosity" and the local velocity gradient.

Computational fluid dynamics is becoming a more important field as memory capacities grow bigger, computers get quicker, and numerical

algorithms get better. Accurate prediction of flows minimizes the amount of wind tunnel testing and helps the designer to make better designs. Two "state-of-the-art" programs for predicting flows and boundary layers in a cascade the Q3DFLOW-81 and a CEBCAS are examined. The Q3DFLOW-81 is a turbomachinery program developed by Dr. Hirsch and associates of the Free University of Brussels [Ref. 4] and [Ref. 5]. The blade-to-blade portion is used to calculate inviscid incompressible flows in a cascade. Inviscid results are presented for several airfoils/blades and configurations. Experimental data, analytical solutions or other computational flow data are compared where applicable. The CEBCAS is a standard Cebeci two-dimensional, incompressible and constant viscosity boundary layer program modified to give graphical output for boundary layer and skin friction distribution and calculate losses and drag coefficients for airfoils/blades in cascade. The CEBPLT is also a standard Cebeci two-dimensional, incompressible and constant viscosity boundary layer program modified to give graphical output for boundary layer and skin friction distribution and calculate drag coefficients for isolated airfoils. CEBPLT and CEBCAS are used to calculate boundary layers on several isolated airfoils and airfoil/blades in a cascade. Experimental data is correlated when available and reasonable to do so. Additionally, the theory and operation of the Cebeci boundary layer programs (Chapter III. and Appendix A respectively) are presented.

II. INVISCID FLOW COMPUTATIONS IN A CASCADE

Physical flow is three dimensional and unsteady, especially in an axial flow compressor. Simplification of this complex flow in a compressor is usually approached by splitting it into two two-dimensional flows:

1. The meridional flow
2. The cascade flow (sometimes referred to as the blade-to-blade)

Solution to the flow in the cascade plane is input for the meridional "through flow" solution, which makes the accurate prediction of flow in the cascade plane very important. Gostelow [Ref. 6: p. 86] has attributed systematic advances in blade design to the ability to calculate flows in a cascade.

Inviscid flow computations in a cascade are indeterminate for practical turbomachine blades. The outlet condition, usually the outlet angle, is specified and at present is found experimentally. For isolated airfoils the Kutta condition gives meaningful results at small angles of attack for practical shapes (that is airfoil shapes that have relatively sharp trailing edges). However, most practical turbomachinery blades have trailing edges that are rounded so as to avoid stresses and manufacturing problems. Frequently, laminar flow will separate near the leading edge and reattach turbulently downstream. This further complicates the modelling process of the flow. Using only an inviscid model it is very difficult to predict the flow. Miller and Serovy [Ref. 7] examined five different trailing edge hypotheses to determine the deviation angle for cascades using the inviscid model. None of the five trailing edge conditions tested were considered acceptable as a general rule such as the Kutta condition is for sharp trailing edges. This is understandable since the outlet angle is influenced by viscous effects and on a round trailing edge the determination of a rear stagnation point is not as easy as on a sharp trailing edge. Gostelow [Ref. 8] reported in a particular example solved by exact potential flow

theory that a change in rear stagnation point location of as little as .3% of the chord would change the outlet angle by as much as 10 degrees. Also, the precise location of the rear stagnation point at some incidence is not necessarily the "correct" location for some other incidence.

A. Q3DFLOW-81 (BLADE-TO-BLADE MODULE)

The Q3DFLOW-81 is a turbomachinery program for calculating flows in an axial flow compressor or turbine. This program uses a finite element method. The blade-to-blade module was used to solve the inviscid equations for flow in a cascade. Substantial runs were made with the Q3DFlOW-81 program for various compressor blades (including even sharp trailing edge airfoils) in a cascade. In order to compare with experimental data each configuration was run twice, one time with outlet angle specified by the experimental angle and another with the Kutta condition option.

The major problem encountered in running the Q3DFLOW was in generating an acceptable finite element mesh. The finite element mesh generation appeared to be very sensitive to the placement of coordinates used to define the shape of the airfoil/blade, especially around the leading edges and trailing edges. Observations of running Q3DFLOW (blade-to-blade) indicate a need for a close one-to-one correspondence between lower and upper coordinates of the surface of the airfoil, say within one to three percent of chord (i.e. the streamwise direction) for the major portion of the airfoil and closer for leading and trailing edge if rounded. The more curvature in the airfoil geometry the smaller the spacing between adjacent coordinates needed to define the geometry to ensure that flow computations are for the right shape. However, too many points to define the leading edges or rounded trailing edges will generate erroneous mesh elements. A general rule of thumb is to use the minimum points needed for the eye/brain to generate the correct airfoil shape by mentally connecting coordinates.

Four parameters ILWIN, IVPIN, ILWOUT, and IVPOUT of CARD NR B-03 of users guide [Ref. 9] are very useful in solving finite element

mesh problems. These parameter modified the mesh around the leading and trailing edges by forming a triangle element instead of the normal rectangular shaped elements(Figure 2.1). Two other parameters that are sometimes useful are NSTUP of CARD NR B-01 (number of stations in the upstream) for solving leading edge mesh problems and NSTDWN of CARD NR B-01 (number of stations in the downstream) for trailing edge problems (Figure 2.1). A "last ditch maneuver" is to input different coordinates to define the airfoil/blade shape.

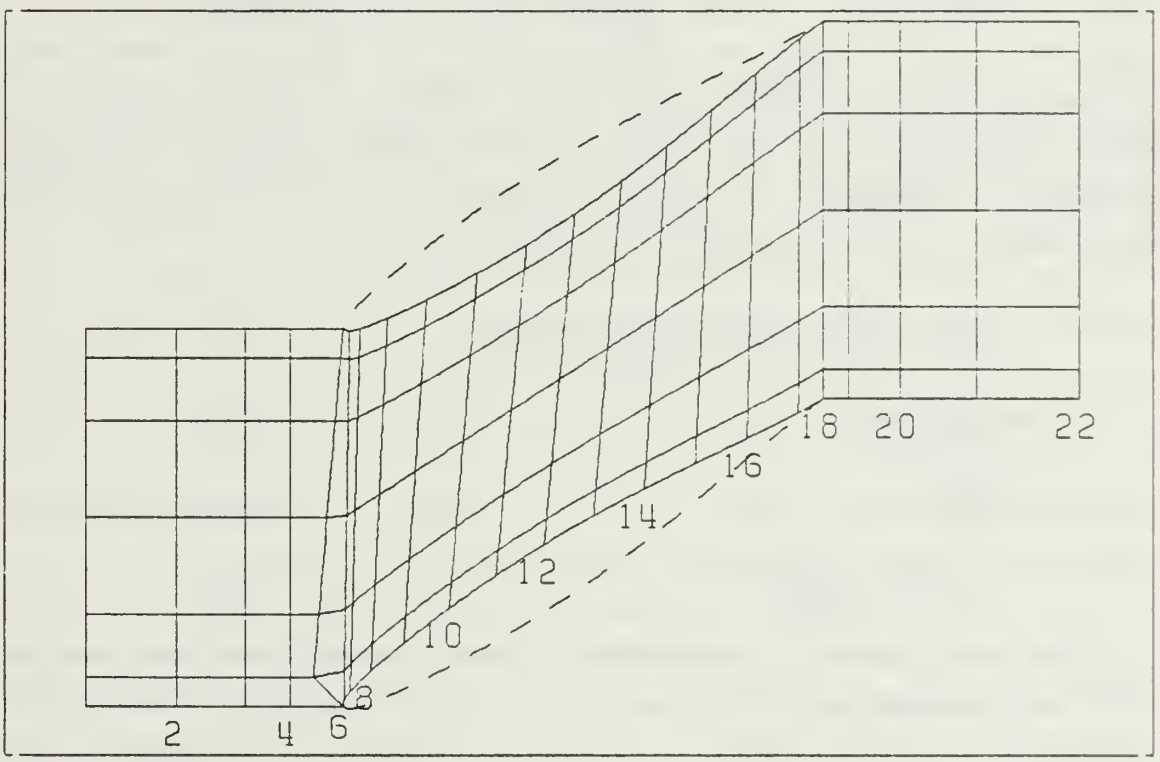

Figure 2.1 Finite Element Mesh
ILWIN =1 ,NSTUP=5,NSTDWN=4

III. THEORY OF CEBECI BOUNDARY LAYER PROGRAM

The governing equations (Eqs. 1, 2 and 3) of the Cebeci two dimensional boundary layer program are obtained from an engineering simplification of the two dimensional Navier Stokes equations by neglecting small terms due to the known empirical fact that the displacement thickness is very small compared to the characteristic length of the airfoil. These equations are then assumed to be applicable to turbulent flows by including only the Reynolds shear stress and neglecting the two Reynolds normal stresses that are obtained by time averaging the two dimensional Navier Stokes equations. Reynolds stresses are essentially empirically obtained and can be expressed in many different forms, depending on the theory used.

$$u\frac{\partial u}{\partial x}+v\frac{\partial u}{\partial y}=-\frac{1}{\rho}\frac{\partial p}{\partial x}+\frac{1}{\rho}\frac{\partial}{\partial y}\left(\mu\frac{\partial u}{\partial y}-\rho\overline{u'v'}\right) \qquad \text{Eq. 1}$$

$$\frac{\partial u}{\partial x}+\frac{\partial v}{\partial y}=0 \qquad \text{Eq. 2}$$

$$\frac{\partial p}{\partial y}=0 \qquad \text{Eq. 3}$$

$$-\rho\overline{u'v'}\equiv\rho\epsilon_{m}\frac{\partial u}{\partial y} \qquad \text{Eq. 4}$$

The eddy viscosity formulation is used in the Cebeci program to model the Reynolds shear stress. This concept was first introduced by Boussinesq in 1877 [Ref. 2: p. 578] in which the turbulent shear stresses are assumed to be similar in nature to the laminar shear stresses and are therefore proportional to the velocity gradient (Eq. 4). Cebeci and Smith [Ref. 10: pp. 255-257] have formulated a two-range empirical eddy viscosity model. In the inner region the formula is similar to the Prandtl mixing length formula modified by a Van Driest damping parameter and intermittency factor that accounts for the transitional region. The outer region is modelled as proportional to an empirical constant, the velocity at the edge, the displacement thickness, and also to the intermittency factor.

Assuming constant density and viscosity and using definitions as stated in Eqs. 5 and 6, Eq. 1 becomes Eq. 7. For laminar flows b is equal to one. Also b may be redefined so that Eq. 7 is useful for axisymmetric laminar flows (Mangler Transformation) with small transverse curvature effect [Ref. 3: p. 48-50].

$$\epsilon_m^+ \equiv \epsilon_m / \nu \qquad \text{Eq. 5}$$

$$b \equiv 1 + \epsilon_m^+ \qquad \text{Eq. 6}$$

$$u\frac{\partial u}{\partial x} + v\frac{\partial u}{\partial y} = -\frac{1}{\rho}\frac{\partial p}{\partial x} + b\nu\frac{\partial^2 u}{\partial y^2} + \frac{\partial b}{\partial y}\frac{\partial u}{\partial y} \qquad \text{Eq. 7}$$

Since the rate of change of local static pressure in the y direction is simplified to equal zero (Eq. 3) and the velocity at the edge of the boundary layer (that is when y is equal to the displacement thickness) is a function of x only, then the Bernoulli equation (Eq. 8) may be used to determine the rate of change of local static pressure in the x direction, as the value in the free stream and surface are considered equal. Differentiating Eq. 8 with respect to x gives Eq. 9. (Note that Eq. 9 is now a differential vice partial since the local static pressure is a function of x only.) The local static pressure is now specified as a pressure coefficient, velocity ratio, etc. from the inviscid/potential solution as a boundary condition for the boundary layer equations. With Eq. 9 ,the simplified momentum equation in the x direction (Eq. 7) and the continuity equation (Eq. 2) reduce to a system of two partial differential equations with two unknowns u and v for laminar flows.

$$p + \frac{1}{2}\rho u_e^2 = \text{const} \qquad \text{Eq. 8}$$

$$\frac{dp}{dx} = -\rho u_e \frac{du_e}{dx} \qquad \text{Eq. 9}$$

The Falkner-Skan transformation (Eq. 10) defines a dimensionless coordinate η and Eq. 11 defines a stream function ψ which consist of a dimensionless stream function f in x and η. A necessary and sufficient condition for the existence of a stream function is that continuity (Eq. 2) be satisfied and hence Eqs. 12 and 13 must be satisfied. This

transformation along with the definition of a stream function and use of the chain rule for differentiating reduces Eqs. 7 and 2 into one partial differential equation with one unknown stream function in η and x for laminar flows with no known analytical solution . For similar flows this transformation changes a system of two partial differential equations into one ordinary differential equation with an unknown stream function as a function of the independent variable η.

$$\eta \equiv \left(\frac{u_e}{\nu x}\right)^{1/2} y \qquad \text{Eq. 10}$$

$$\psi \equiv (u_e \nu x)^{1/2} f(x, \eta) \qquad \text{Eq. 11}$$

$$u = \frac{\partial \psi}{\partial y} \qquad \text{Eq. 12}$$

$$v = -\frac{\partial \psi}{\partial x} \qquad \text{Eq. 13}$$

Similar flows are laminar flows that satisfy Eq. 14. An example of a similar flow is the flow over the flat plate. In this example the pressure-gradient parameter, m is equal to zero. The definition of m (Eq. 15) may be derived by differentiating Eq. 14 by x ,substituting Eq. 14 back into this differentiated equation, and then solving for m. The concept of similarity is not as important now as it was before the advent of the computer. It allowed for practical numerical solutions of certain flows even though very few of the flows can model any real world phenomenon. For further understanding of the concept of similarity see References 2 and 3.

$$u_e = Cx^m \qquad \text{Eq. 14}$$

$$m = \frac{x}{u_e}\frac{du_e}{dx} \qquad \text{Eq. 15}$$

Derivation of Eq. 22 is a simple matter of putting u , v and their partial derivatives in terms of the dimensionless stream function f by using Eqs. 10-13 and the chain rule. (For example Eq. 16 gives Eq. 17, where prime denotes partial differential with respect to η). Eqs. 17-21 show the results of this. Substituting Eqs. 17-21 into Eq. 7,

rearranging , expanding, and multiplying the equation by x and dividing by u_e squared, and then substituting in the pressure gradient parameter (Eq. 15), Eq. 22 may be obtained for non-similar laminar flows (b=1). Now b is a function of η and must be written as Eq. 23 to account for turbulent flows.

$$u = \frac{\partial \psi}{\partial y} = (u_e \nu x)^{1/2} \frac{\partial f}{\partial \eta} \frac{\partial \eta}{\partial y} \qquad \text{Eq. 16}$$

$$u = u_e f' \qquad \text{Eq. 17}$$

$$v = -\frac{f}{2}\left(\left(\frac{\nu x}{u_e}\right)^{1/2} + \left(\frac{u_e \nu}{x}\right)^{1/2}\right) - (u_e \nu x)^{1/2} \frac{\partial f}{\partial x} \qquad \text{Eq. 18}$$

$$\frac{\partial u}{\partial x} = \frac{d u_e}{d x} f' + u_e \frac{\partial f'}{\partial x} \qquad \text{Eq. 19}$$

$$\frac{\partial u}{\partial y} = \left(\frac{u_e^3}{\nu x}\right)^{1/2} f'' \qquad \text{Eq. 20}$$

$$\frac{\partial^2 u}{\partial y^2} = \left(\frac{u_e^2}{\nu x}\right) f''' \qquad \text{Eq. 21}$$

$$f''' + \frac{m+1}{2} f f'' + m[1 - (f')^2] = x\left(f' \frac{\partial f'}{\partial x} - f'' \frac{\partial f}{\partial x}\right) \qquad \text{Eq. 22}$$

$$(b f'')' + \frac{m+1}{2} f f'' + m[1 - (f')^2] = x\left(f' \frac{\partial f'}{\partial x} - f'' \frac{\partial f}{\partial x}\right) \qquad \text{Eq. 23}$$

This third order nonlinear partial differential equation (Eq. 23) is written as a system of three first order partial differential equations (Eq. 24-26) by defining two new variables script u and script v functions in η (Eq. 24 and 25 respectively). Script u is a nondimensional x-component velocity but script v has no direct correspondence to the y-component velocity. The three unknowns of this third order system are script u, script v, and f. Recalling Eq. 17 and the fact that the velocity is zero at a solid surface of an airfoil (η=0), the stream function f and its partial derivative with respect to η is equal to zero. Hence two of three boundary conditions needed are Eq. 27 and 28. The third boundary condition (Eq. 29) comes from the velocity at the edge (η= displacement thickness) being modelled equal to the velocity at η equal to infinity for a given x location.

$$f' = u \qquad \text{Eq. 24}$$

$$u' = v \qquad \text{Eq. 25}$$

$$(bv)' + \frac{m+1}{2} f v + m[1-(u^2)] = x\left(u\frac{\partial u}{\partial x} - v\frac{\partial f}{\partial x}\right) \qquad \text{Eq. 26}$$

$$f(x,0) = 0 \qquad \text{Eq. 27}$$

$$u(x,0) = 0 \qquad \text{Eq. 28}$$

$$u(x,\eta_\infty) = 0 \qquad \text{Eq. 29}$$

Cebeci uses central finite differences of truncation error of second order in η on the net rectangle shown in Figure 3.1 and averages at the midpoints of the net. The central finite difference of the first derivative formula (Eq. 32) used in Cebeci's program can easily be derived by use of a Taylor series expansion of a point x+h and a point x-h (Eq. 30 and 31 respectively, see Figure 3.2). Eq. 32 is obtained by subtracting Eq.31 from Eq.30 and then solving for the first derivative.

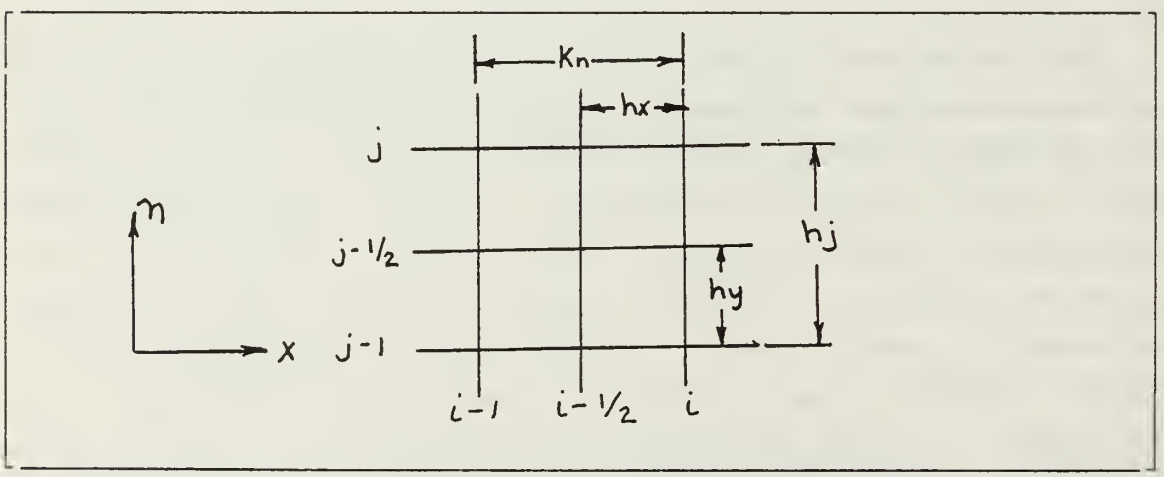

Figure 3.1 Boundary Layer Grid

$$f(x+h)=f(x)+hf'(x)+\text{higher order terms} \qquad \text{Eq. 30}$$

$$f(x-h)=f(x)-hf'(x)+\text{higher order terms} \qquad \text{Eq. 31}$$

$$f'(x)=\frac{f(x+h)-f(x-h)}{2h}+0(h^2) \qquad \text{Eq. 32}$$

The $0(h^2)$ in Eq. 32 represents the sum of the remaining terms of order h^2 in the series. Eq. 29 gives an exact value of the derivative if all terms in the infinite series are retained or if h goes to zero. Since Eq. 29 is truncated by discarding all terms of order h^2 this finite difference formula is of truncation error of order h^2. The spacing between grid points (h) is usually relatively small and the error incurred by this approximation is usually insignificant for most engineering purposes. Central finite differences of the first derivatives are applied at the mid points of the net. Twice the hx and hy distance are defined as kn and hj (that is the x distance between i-1 and i grid location and the η distance between j-1 and j grid location respectively, see Figure 3.1). Rewriting Eq. 32 in terms of subscript sequence grid location numbers i and j of the spanwise and normal direction respectively at the midpoints and accounting for the fact that all derivatives are partial gives Eq. 33 and Eq. 34 respectively. For example, Eq. 33 is the partial derivative of f in the spanwise direction for any constant normal grid location (j). Using Eq. 33 to approximate Eq. 24 and 25 averaging script u and script v at the midpoint in the j direction , and rearranging, Eqs. 35 and 36 are obtained. In a similar manner and with use of the central difference approximation for the partial derivative in the spanwise direction Eq. 26 is transformed from a partial differential equation to an algebraic equation and will not be presented here due to its lengthy derivation and additional definitions introduced that are unnecessary but convenient [Ref. 3: pp. 216 and 217].

$$f'_{i-1/2,j}=\frac{f_{i,j}-f_{i-1,j}}{k_i} \qquad \text{Eq. 33}$$

$$f'_{i,j-1/2}=\frac{f_{i,j}-f_{i,j-1}}{h_j} \qquad \text{Eq. 34}$$

$$f_{i,j} - f_{i,j-1} - \frac{h_j}{2}(u_{i,j} + u_{i,j-1}) = 0 \qquad \text{Eq. 35}$$

$$u_{i,j} - u_{i,j-1} - \frac{h_j}{2}(v_{i,j} + v_{i,j-1}) = 0 \qquad \text{Eq. 36}$$

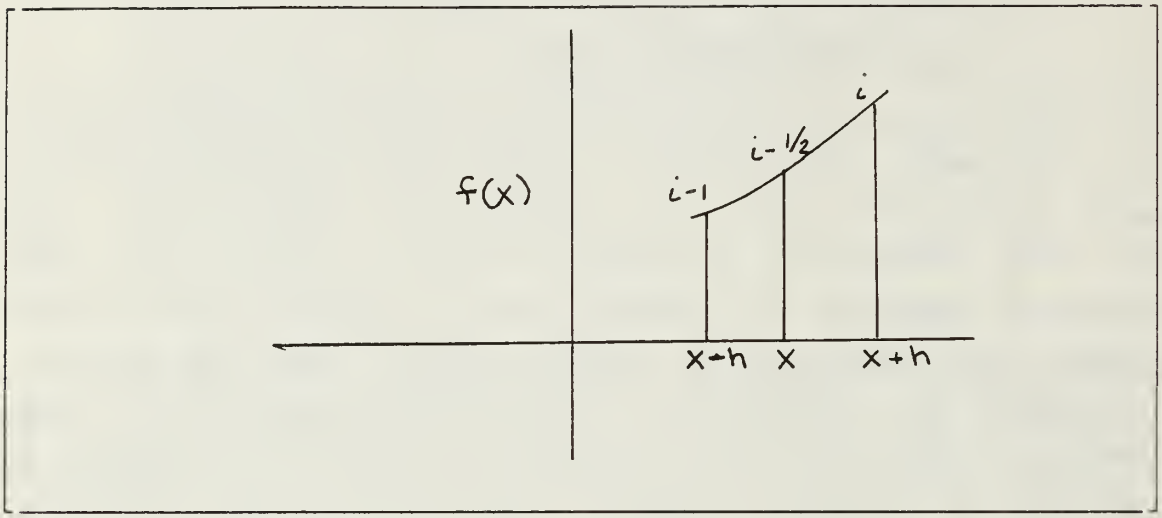

Figure 3.2 Points Defined for Taylor Series Expansion

If all values of f, script u, and script v are known at some initial downstream spanwise grid location, say i-1 for all values of j then Eq. 35 , 36 and Eq. (7.2.10c) of Reference 3 are a nonlinear system (that is the system is nonlinear since the last equation is nonlinear) of 3J+3 equations with 3J+3 unknowns where j=0,1,2,3...,J. Cebeci uses Newton's method to solve this system of nonlinear equations. Cebeci departs slightly from the strict application of Newton's method in treating the b terms of Eq. (7.2.10c) of Reference 3 to avoid unnecessary complication [Ref. 11]. The solution to this now linearized set of equations is accomplished by a very efficient block elimination method which is possible due to the unique form that the system of equation can be put in. This method is fairly elaborate and will not be presented here.

The basic idea of Newton's method can be understood from a little geometry. Suppose we wish to solve for the roots of this nth order polynomial in the independent variable x where n is greater than 1 and hence nonlinear. Say this polynomial f(x) is defined as in Figure 3.3 .

Now suppose we guess a solution to one of the roots of this polynomial say x1. From geometry, the tangent of θ is f(x1)/x1-x2 which is also the slope at x1 that is f'(x1). Solving for x2 and writing in terms of sequence iteration numbers for successive approximations we obtain Eq. 37. An exact value to this root can not be given with only a finite number of iterations so an acceptable convergence limit is usually defined between successive iterations. Cebeci considers the wall shear parameter that is f'' at η equal to zero (also known as script v) as the greatest source of errors in boundary layer equations. The convergence criterion is .00001 between successive iterations of the wall shear parameter (f''(0)) for laminar flows. For turbulent flows the convergence criterion is expressed as a percentage. There are many problems that can be encountered by this technique. For instance if the initial guess is "poor" this technique may converge to a root not sought or may not even converge at all. However, due to the nature of the boundary layer equations and the manner in which Cebeci applies it, Newton's method is "unconditionally stable" For a more detailed discussion of the theory of Cebeci boundary layer program see Reference 3.

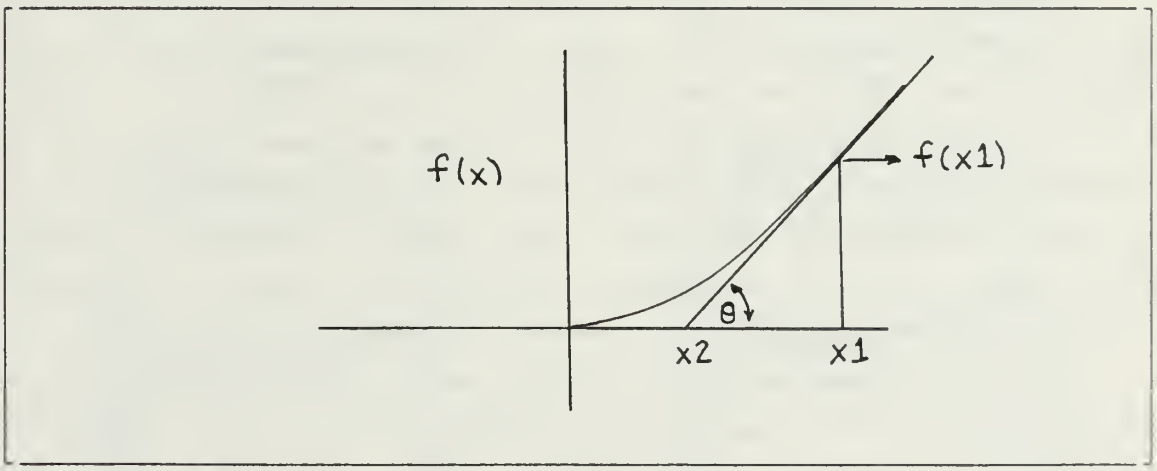

Figure 3.3 Newton's Method

$$x_{i+1} = x_i - \frac{f(x_i)}{f'(x_i)} \qquad \text{Eq. 37}$$

IV. RESULTS OF Q3DFLOW INVISCID BLADE-TO-BLADE COMPUTATIONS

Several blade shapes and configurations were run using the blade to blade portion of the Q3DFLOW-81 program. Several different graphical outputs are available from Q3DFLOW, but only those that could be compared with other available information are presented here. Results are presented in graphical output usually as pressure coefficients.

A no camber, sharp trailing edge airfoil, the NACA 65-010 (see Appendix B for shape and coordinates used to input Q3DFLOW) was run at an inlet $\beta = 30°$, $\sigma = 1.5$, and several α's. Figure 4.1 shows the results of the Q3DFLOW-81 blade to blade (solid line) plotted as a pressure coefficient vs. chord. The circle and triangle points depict the experimental pressure coefficients obtained from NACA TN 3916 [Ref. 12]. Figure 4.1 shows the results specifying the experimental outlet β as given in NACA TN 3916. Figure 4.2 shows results using the Kutta condition.

A slightly cambered, rounded trailing edge blade, the NACA 65-($4A_2$ I_{8b})10 (see Appendix C for shape and coordinates used to input Q3DFLOW) was run at an inlet $\beta = 30°$, $\sigma = 1.0$ and several α's. Figure 4.3 shows the results of Q3DFLOW-81 blade to blade (solid line) as pressure coefficient vs. chord when specifying the experimental outlet β as given in NACA TN 3817 [Ref. 13]. Figure 4.4 shows the results when using the Kutta condition. Experimental pressure coefficients (circles and triangles) obtained from NACA TN 3817 are also plotted.

A slightly cambered, sharp trailing edge airfoil, the NACA 8410 (see Appendix D for shape and coordinates used to input Q3DFLOW) was run at an inlet $\beta = 44.4°$ and $\sigma = 1.33$. Figure 4.5 shows the results of Q3DFLOW-81(solid line) using the Kutta condition, as velocity ratios referenced to the approach velocity vs. chord. The velocity ratios, as calculated by the Schlichting-Method and given by AGARD-AG-220 [Ref. 14: pp. 317-319], are referenced to the approach

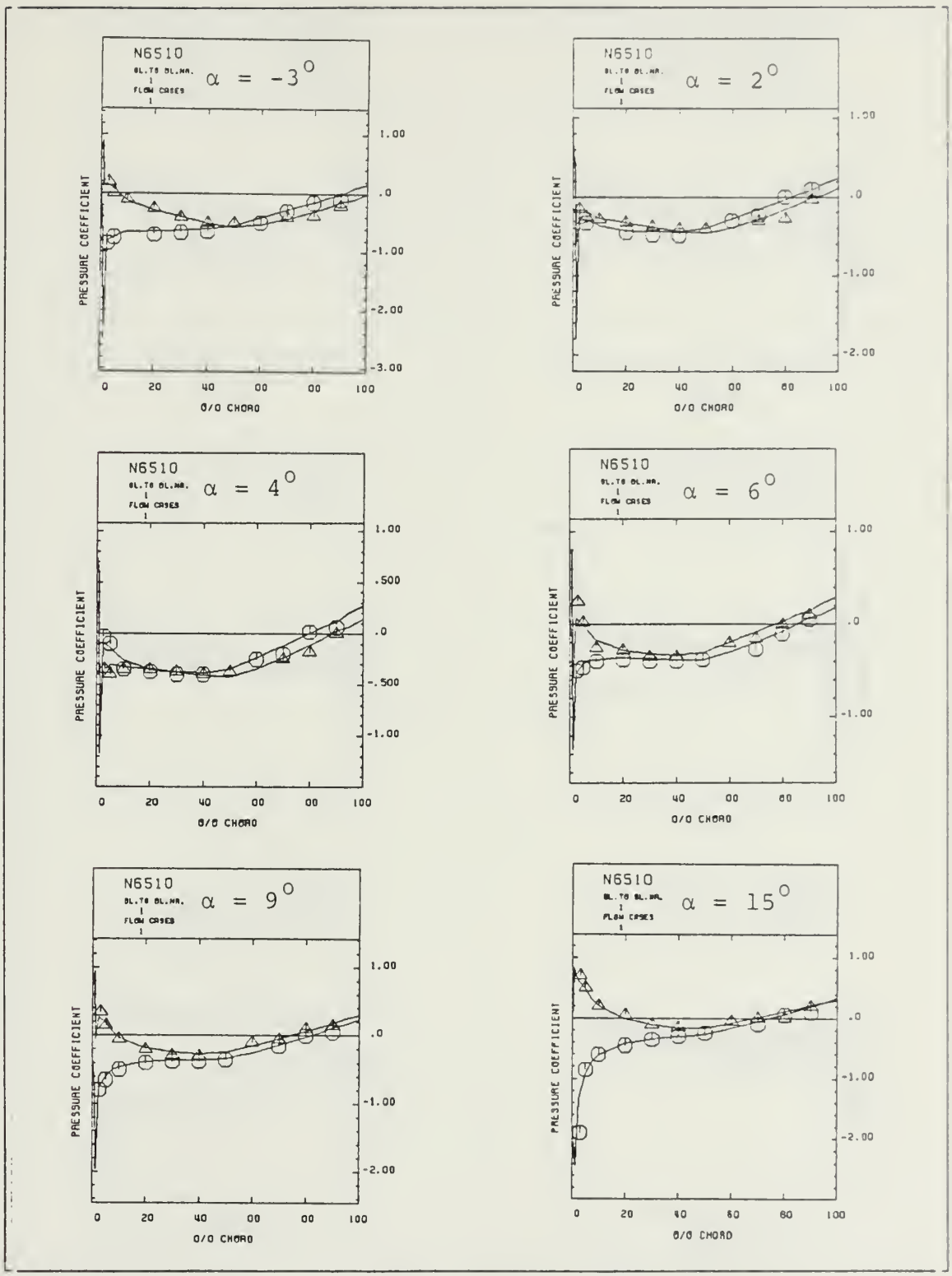

Figure 4.1 Q3DFLOW Results for NACA 65-010
(Outlet β Given from Experiment)

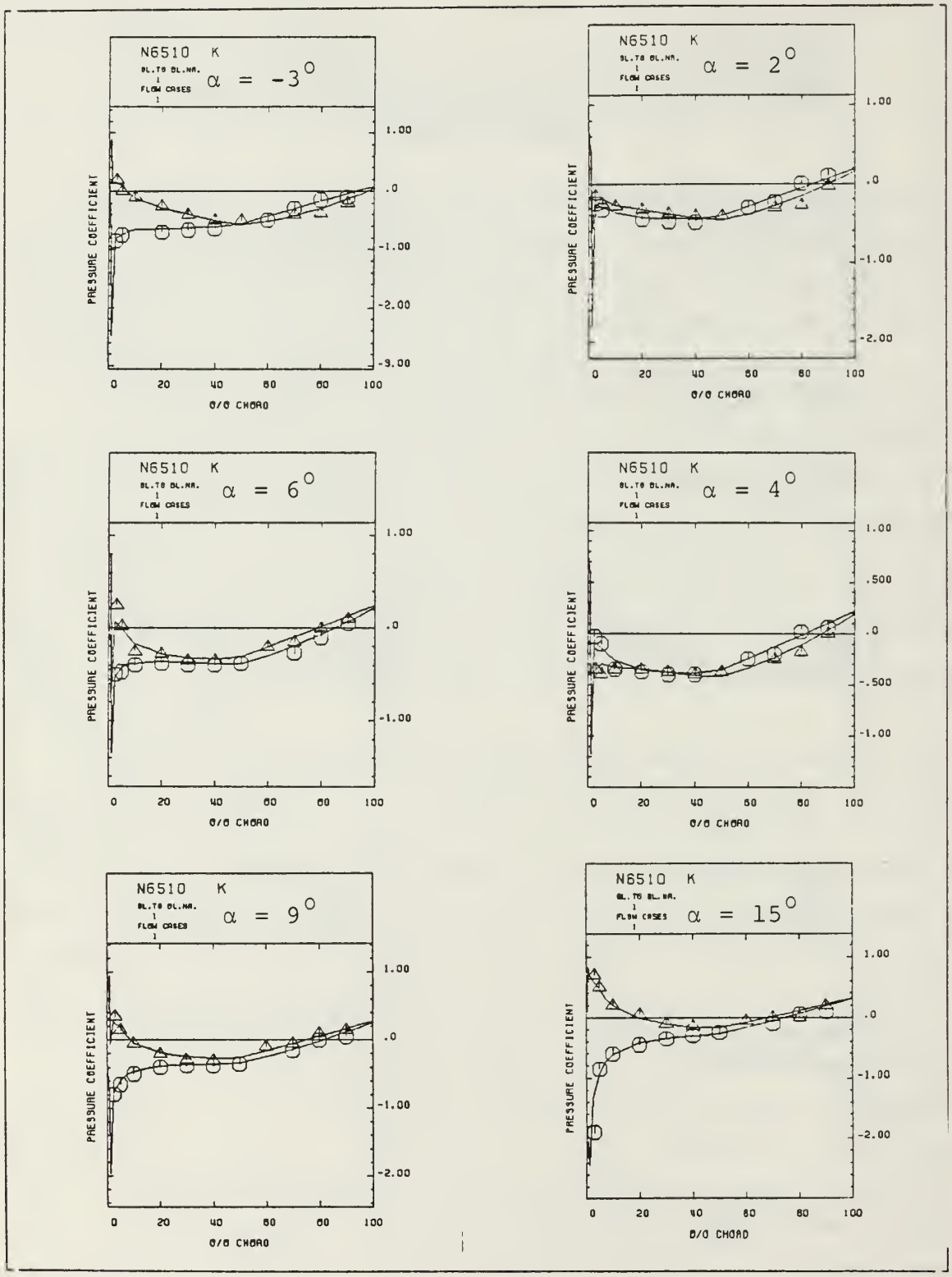

Figure 4.2 Q3DFLOW Results for NACA 65-010 (Kutta Condition)

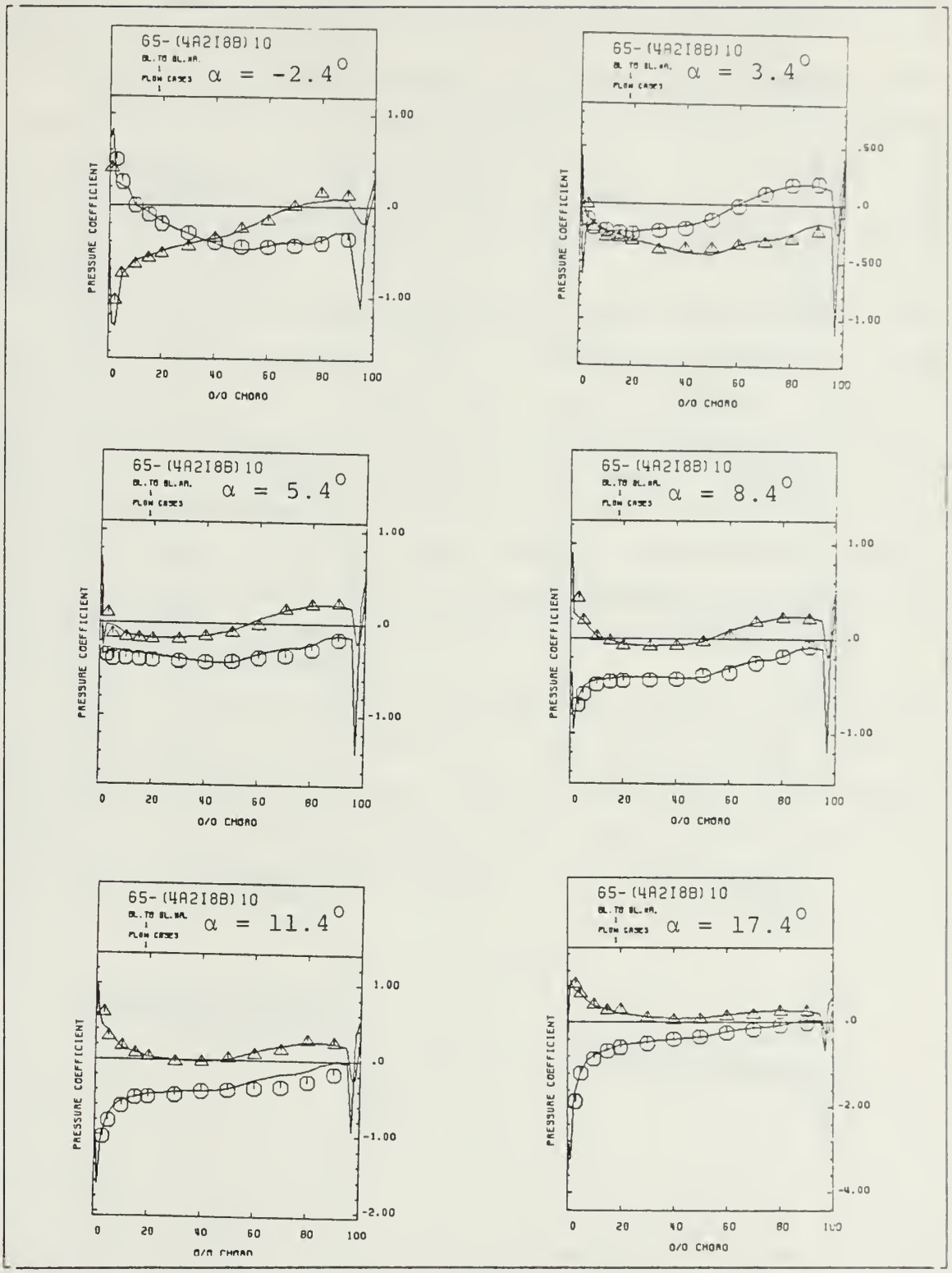

Figure 4.3 Q3DFLOW Results for NACA 65-($4A_2I_{8b}$)10
(Outlet β Given from Experiment)

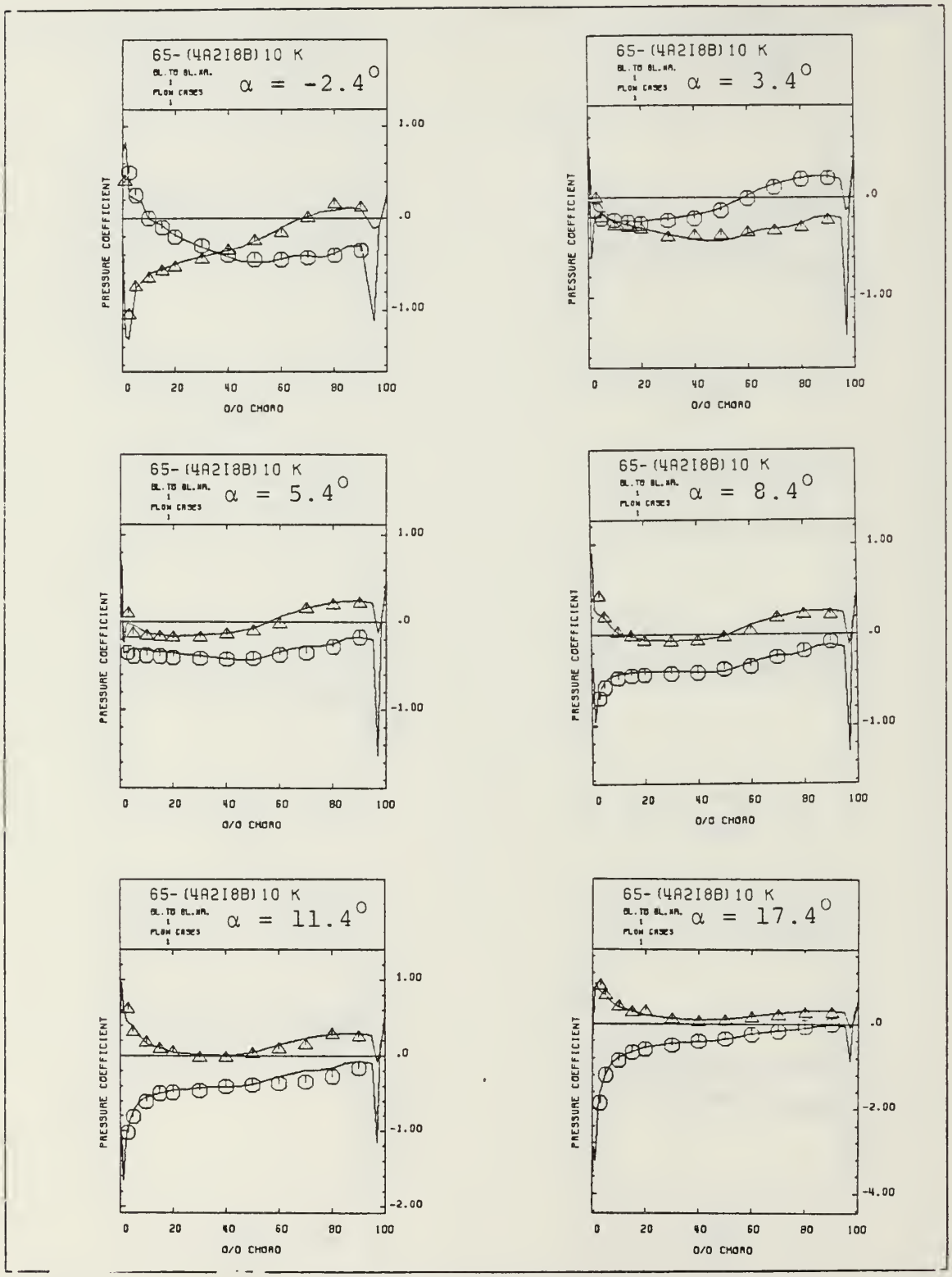

Figure 4.4 Q3DFLOW Results for NACA 65-$(4A_2I_{8b})$10 (Kutta Condition)

velocity vice the mean velocity as originally given and are presented as circles and triangles in Figure 4.5 .

A cusped blade (see Appendix E for shape and coordinates used to input Q3DFLOW) from Gostelow [Ref. 6: pp. 109,110,123,124] was run at an inlet β = 37.5° and σ =1.01. Figure 4.6 shows results as pressure coefficient vs. per cent chord using the Kutta condition. The circles and triangles on Figure 4.6 show the results as analytically determined by Gostelow.

An advanced controlled-diffusion fan blade (see Appendix F for shape) was run at an inlet β = 68°, γ = 58.25° ,σ = 1.34 and an axial velocity/density ratio (AVDR)=1.443. Figure 4.7 shows results of Q3DFLOW-81 as pressure coefficient vs. chord (solid line) using the experimental outlet angle as measured in the cascade wind tunnel at the Turbopropulsion Laboratory of the Naval Postgraduate School. Figure 4.8 shows results using the Kutta condition. Experimental pressure coefficients as measured in the cascade wind tunnel at the Turbopropulsion Laboratory of the Naval Postgraduate School are plotted as circles and triangles.

Table I shows outlet β as calculated from Q3DFLOW using the Kutta condition option for all blades run. The Kutta condition option of Q3DFLOW uses an initial outlet β which was given as the experimental outlet β or other analytical outlet β. Also shown is outlet β given from experiment or another available method.

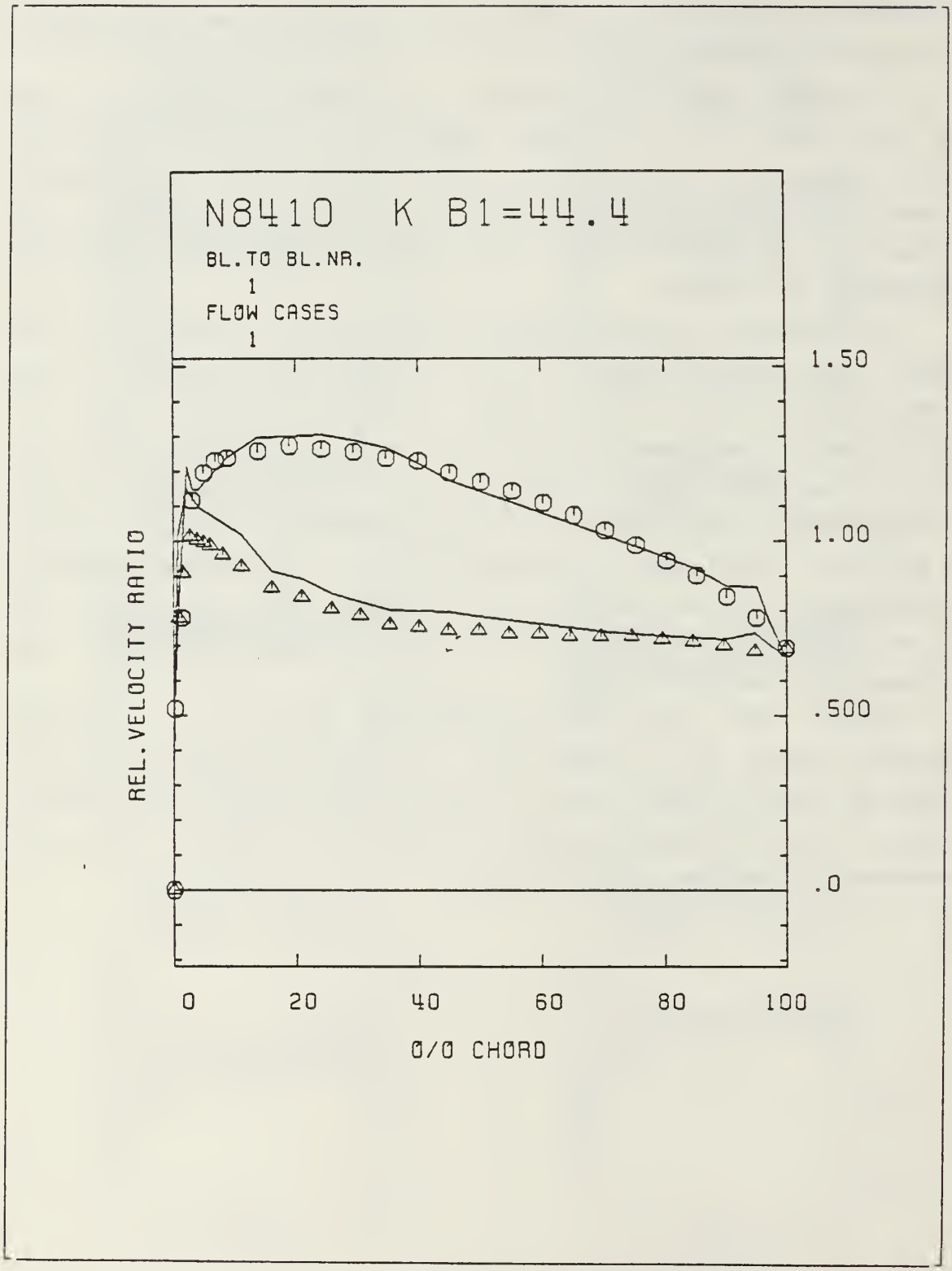

Figure 4.5 Q3DFLOW Results for NACA 8410 (Kutta Condition)

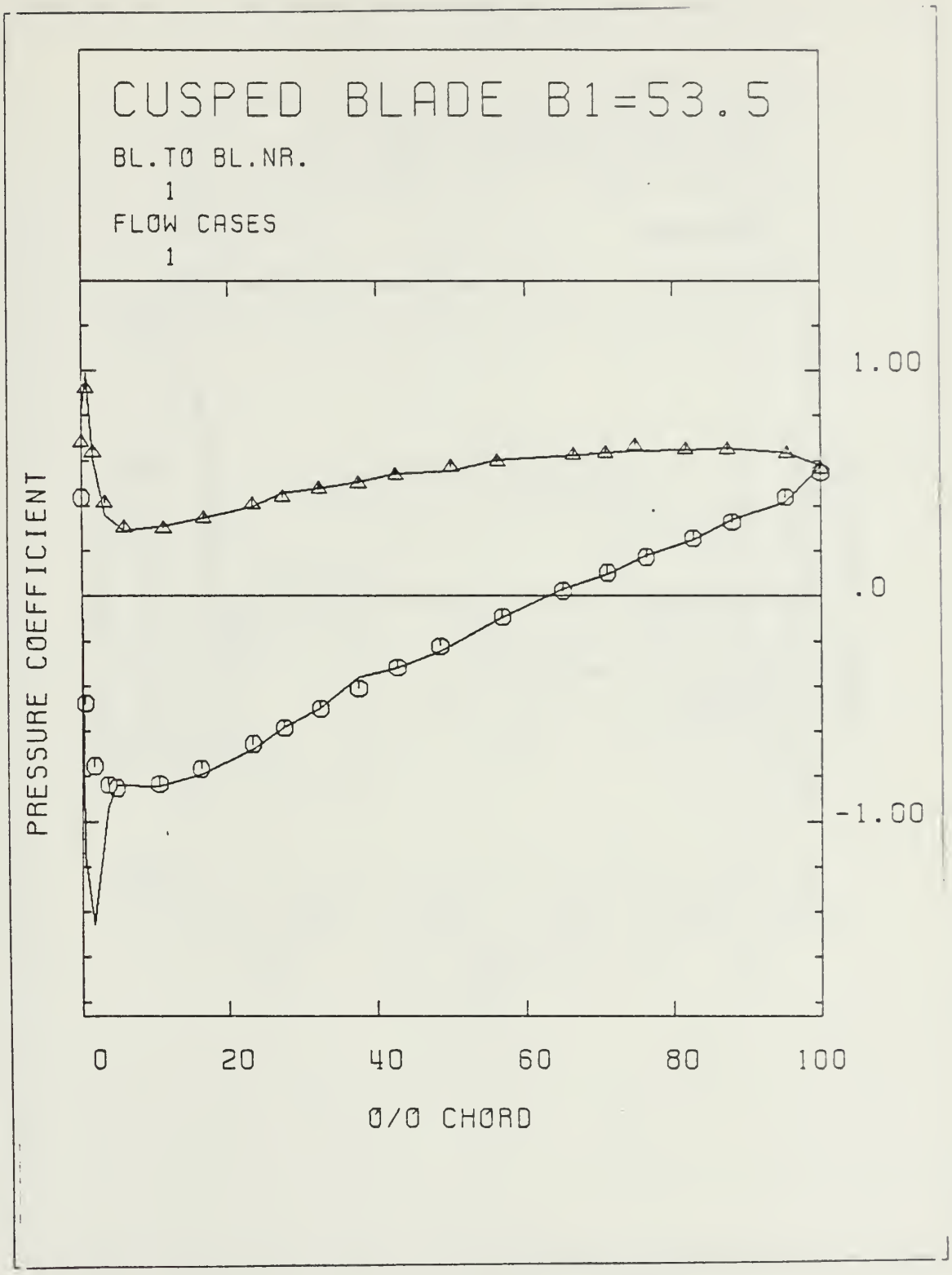

Figure 4.6 Q3DFLOW Results for Cusped Blade (Kutta Condition)

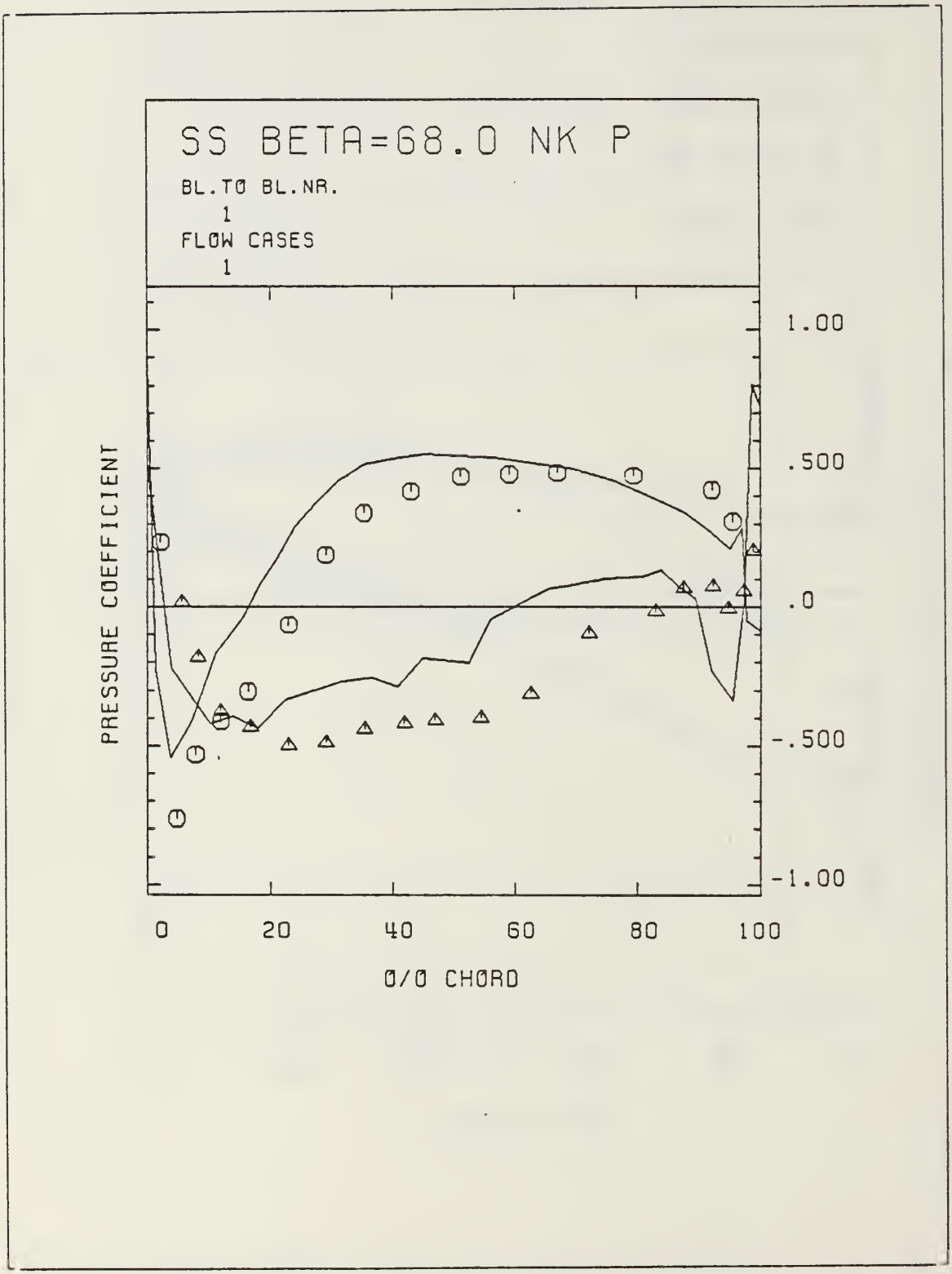

Figure 4.7 Q3DFLOW Results for Fan Blade
(Outlet β 2 Given from Experiment)

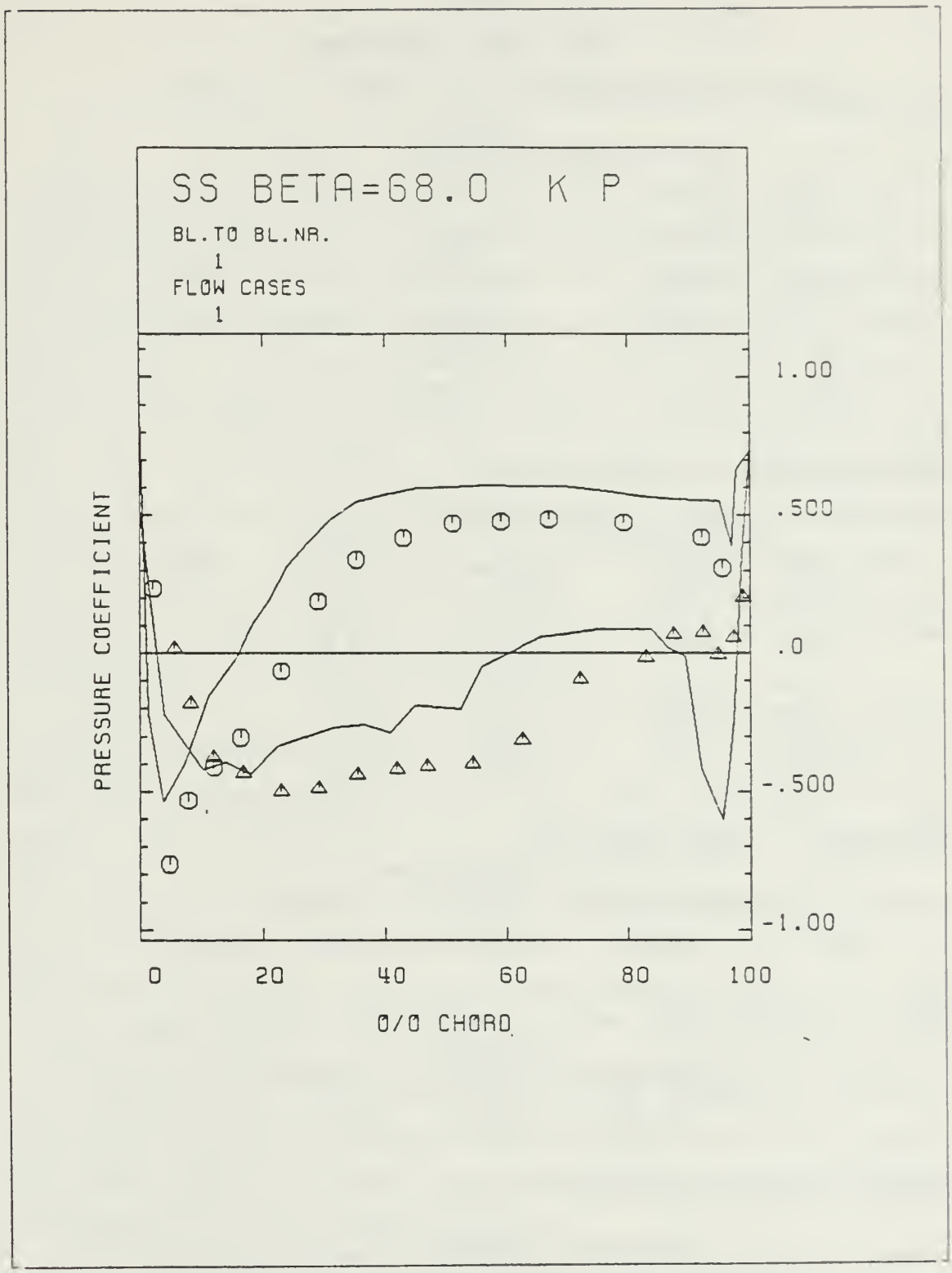

Figure 4.8 Q3DFLOW Results for Fan Blade (Kutta Condition)

TABLE I

Outlet Angle Comparison

NACA 65-010 INLET β=30° σ= 1.5

α	EXPERIMENTAL	Q3DFLOW KUTTA	% DIFF
-3.°	33.9°	34.77°	2.6
2.°	28.7°	29.48°	2.7
4.°	26.6°	27.37°	2.9
6.°	24.6°	25.27°	2.7
9.°	21.7°	21.77°	.3
15.°	16.2°	16.18°	.1

NACA 65-(4A I)10 INLET β=30° σ=1.0

α	EXPERIMENTAL	Q3DFLOW KUTTA	% DIFF
-2.4°	30.2°	29.18°	3.4
3.4°	25.9°	23.43°	9.5
5.4°	21.9°	20.73°	5.3
8.4°	18.9°	17.93°	5.1
11.4°	16.8°	14.83°	11.7
17.4°	11.1°	9.18°	17.3

NACA 8410 INLET β=30° σ=1.0

SCHLICHTING	Q3DFLOW KUTTA	% DIFF
21.3°	20.26°	4.9

FAN INLET β=30° σ=1.0 AVDR=1.43

EXPERIMENTAL	Q3DFLOW KUTTA	% DIFF
48.62°	41.66°	14.3

CUSPED BLADE INLET β=30 σ=1.0

GOSTELOW	Q3DFLOW KUTTA	% DIFF
30.02°	30.02°	0.0

V. RESULTS OF CEBECI BOUNDARY LAYER PROGRAM

Several isolated airfoils were run on CEBPLT. Several airfoils and turbomachinery blades were also run using pressure or velocity distributions from inviscid flow in a cascade (Q3DFLOW-81 blade to blade) as input for CEBCAS. Results from CEBPLT and CEBCAS are presented as graphical output displaying displacement, momentum and skin friction distributions. The velocity distribution input is also displayed. Transition was computed by Michel's method as given by Cebeci and Smith [Ref. 10: pp.332-333] or the point of laminar separation if this occurs first. Drag coefficients on isolated airfoils were calculated using a Squire-Young formula [Ref. 2: pp. 764-765]. Losses were calculated for airfoils/blades in a cascade as given by Roudebush and Lieblein [Ref. 15: p. 24]. The drag coefficient for cascades was calculated by multiplying the losses by the cosine β at infinity (i.e. the β associated with the mean free velocity) and dividing by σ.

NACA 0012 was run using velocity ratios obtained from an inviscid program of the Douglas Aircraft Company at $\alpha = 0°$. NACA 0009 and NACA 0006 were run using inviscid velocity ratios from Abbott and von Doenhoff [Ref. 16] also at $\alpha = 0°$. NACA 4412 was run using the experimental pressure coefficients from Pinkerton [Ref. 4] again at $\alpha = 0°$. Figures 5.1-5.5 show the results of these airfoils as displacement thickness, momentum thickness, and skin friction distributions vs. x/c, fraction of chord. The profile drag coefficient , C_d , and skin friction drag coefficient, C_f , referenced to approach velocity and velocity at the edge, u_e are for one surface only and are given on the skin friction graph. The total profile drag for symmetrical airfoils is twice the C_d value given on skin friction graph at $\alpha = 0°$. Table II shows the comparison between calculated profile drag and measured profile drag as given in [Ref. 16].

The NACA 8410 airfoil was run on CEBCAS using the velocity distribution as given by the Schlichting method in [Ref. 14: pp.

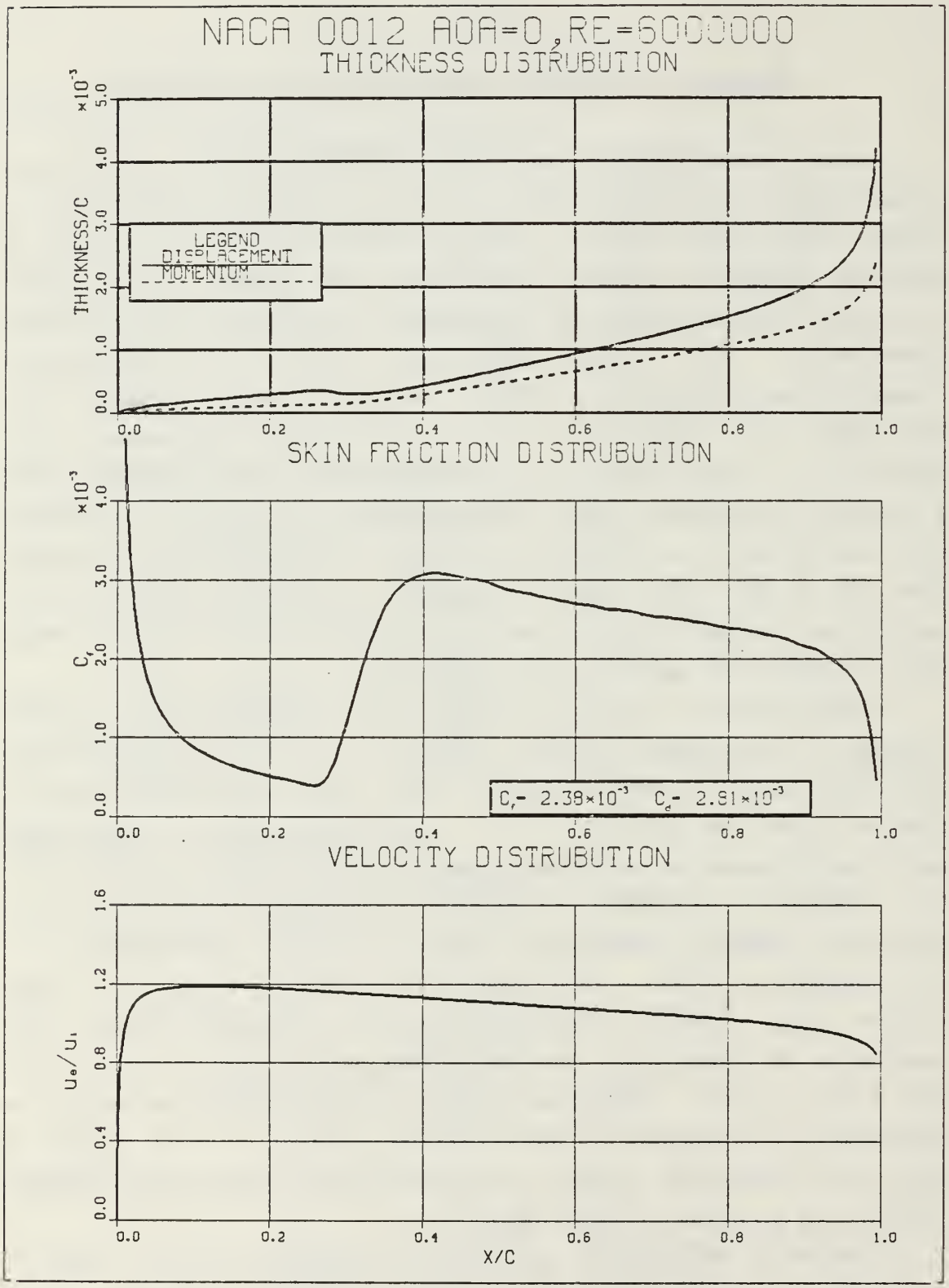

Figure 5.1 NACA 0012 Boundary Layer Results

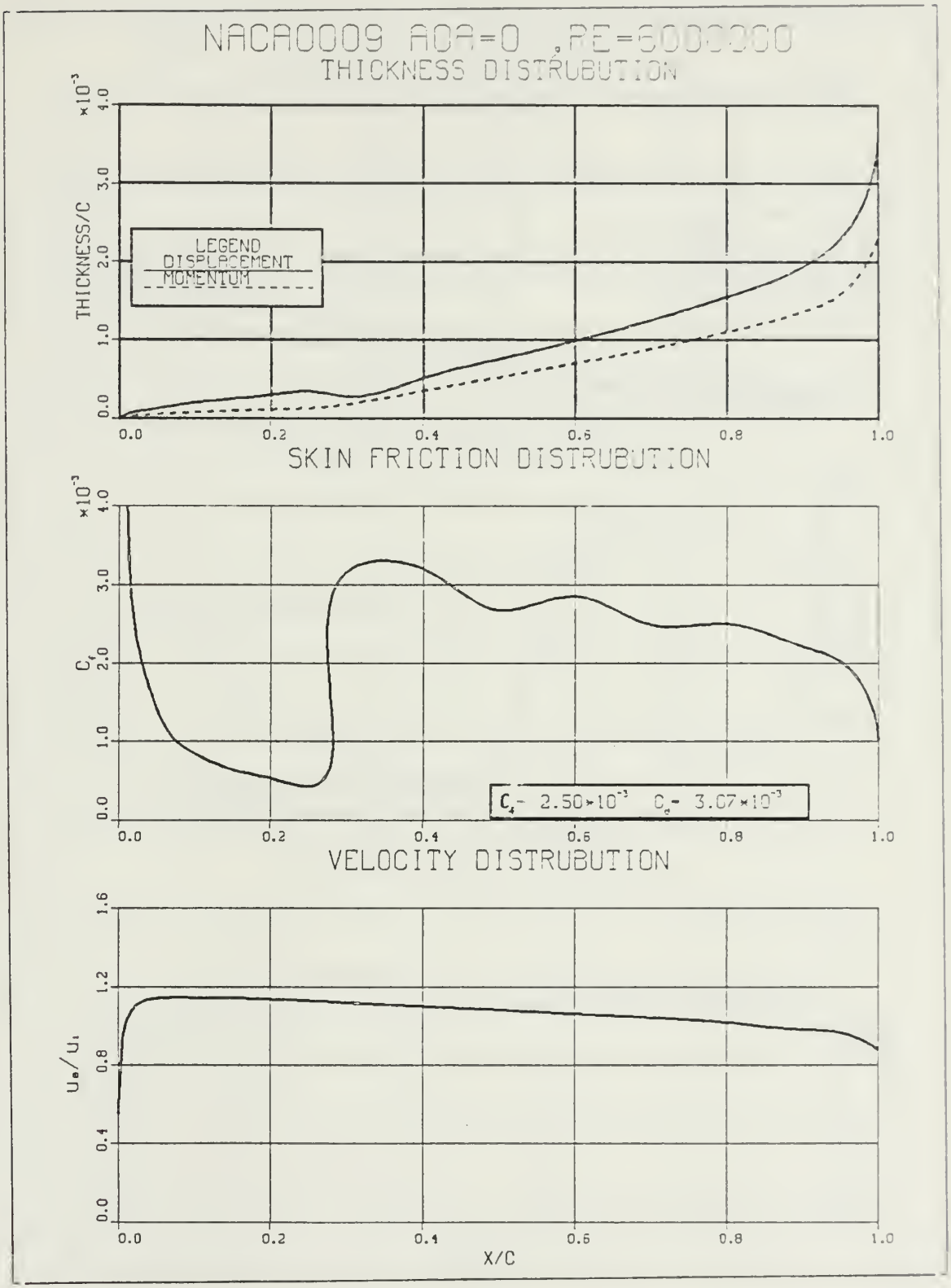

Figure 5.2 NACA 0009 Boundary Layer Results

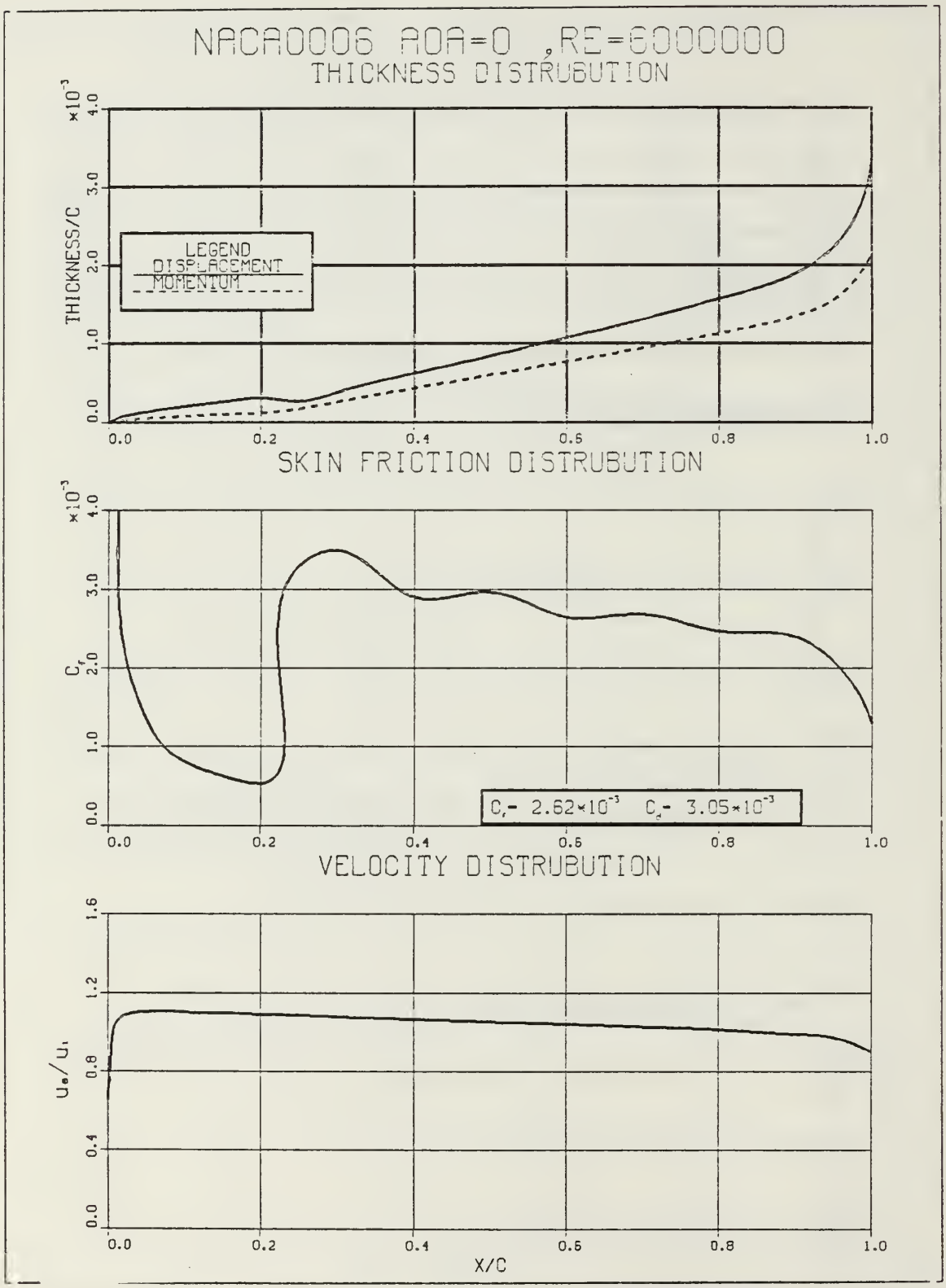

Figure 5.3 NACA 0006 Boundary Layer Results

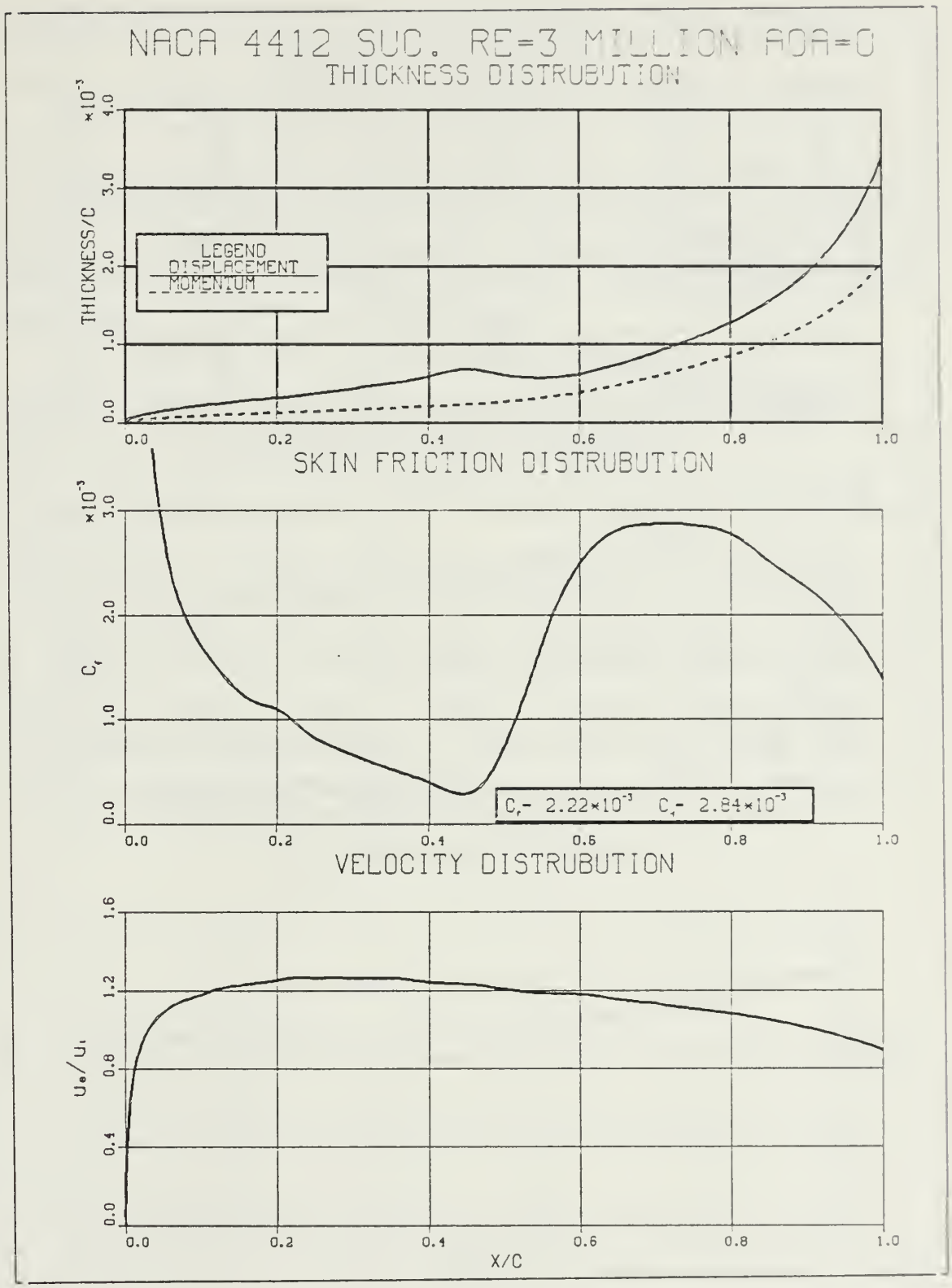

Figure 5.4 NACA 4412 Boundary Layer Results (Suction Side)

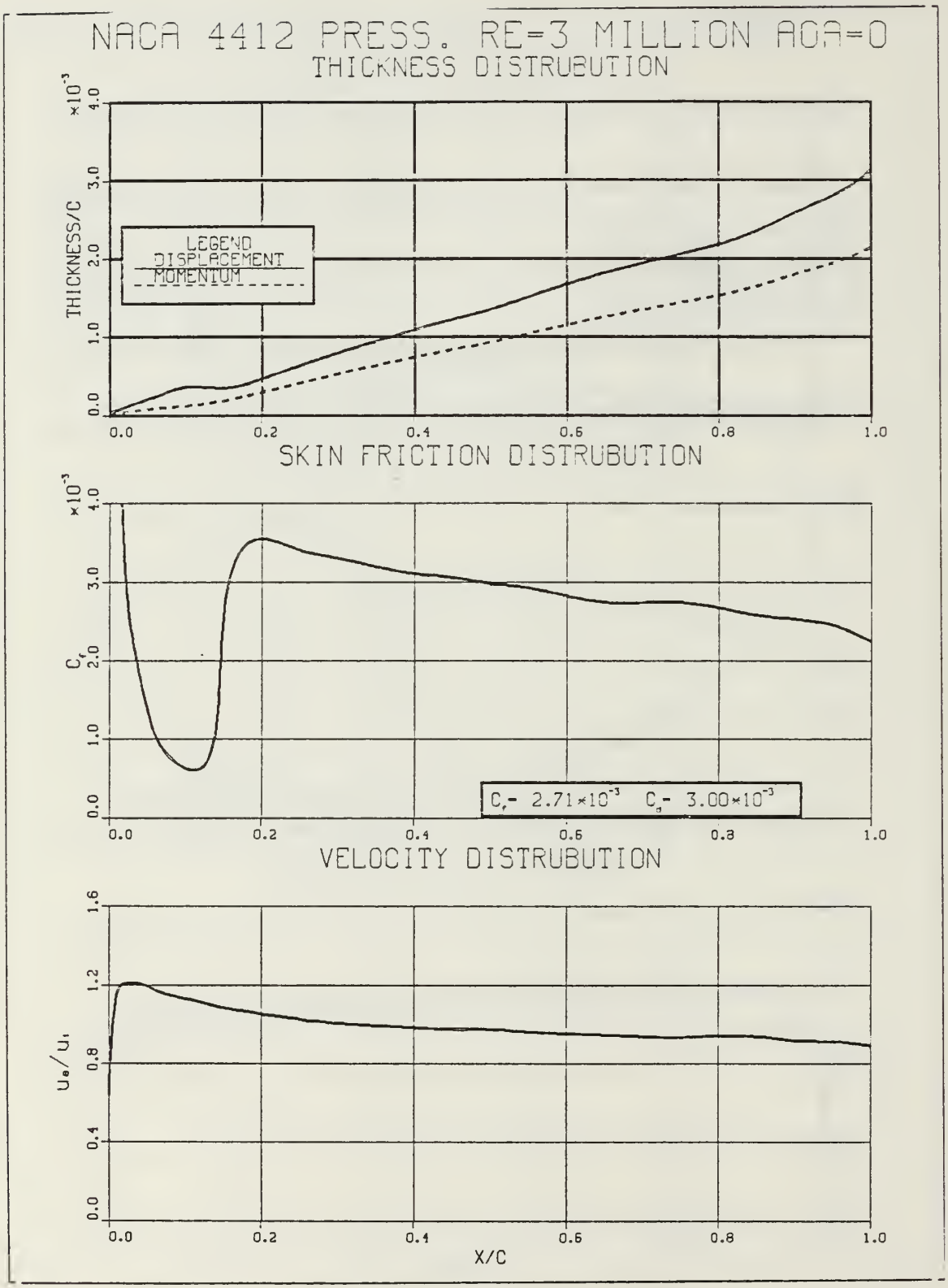

Figure 5.5 NACA 4412 Boundary Layer Results (Pressure Side)

317-318]. after referencing to the approach velocity as input at a Reynolds number of 500,000. Figures 5.6 and 5.7 show results as thickness and skin friction distributions with transition specified as close to the leading edge as possible without incurring a program error. Also shown are the velocity distribution inputs. The displacement and the momentum thickness as calculated with the help of Truckenbrodt's method for a fully turbulent boundary layer as given in [Ref. 14] are plotted as squares and circles, respectively, on the thickness distribution graphs.

The NACA 65-010 and the NACA 65-($4A_2$ I_{8b})10 were run on CEBCAS using the inviscid pressure distribution from Q3DFLOW as input at Reynolds number of 245,000 and 444,000, respectively. Figure 5.8 and 5.9 show results as thickness and skin friction distributions for the NACA 65-010 at an $\alpha = 6°$. The drag coefficient for the cascade referencing to approach velocity as calculated by CEBCAS for the NACA 65-010 at an $\alpha = 6°$ was .0138 as compared to .013 as measured in NACA TN 3916. Table III shows where separation occurs according to CEBCAS in x/c. A "NO" indicates that separation did not occur over forward 95% of chord. Lieblein's equation used for losses does not account for separated flows or blades with round trailing edges and for that reason no other comparisons were made with experimental data.

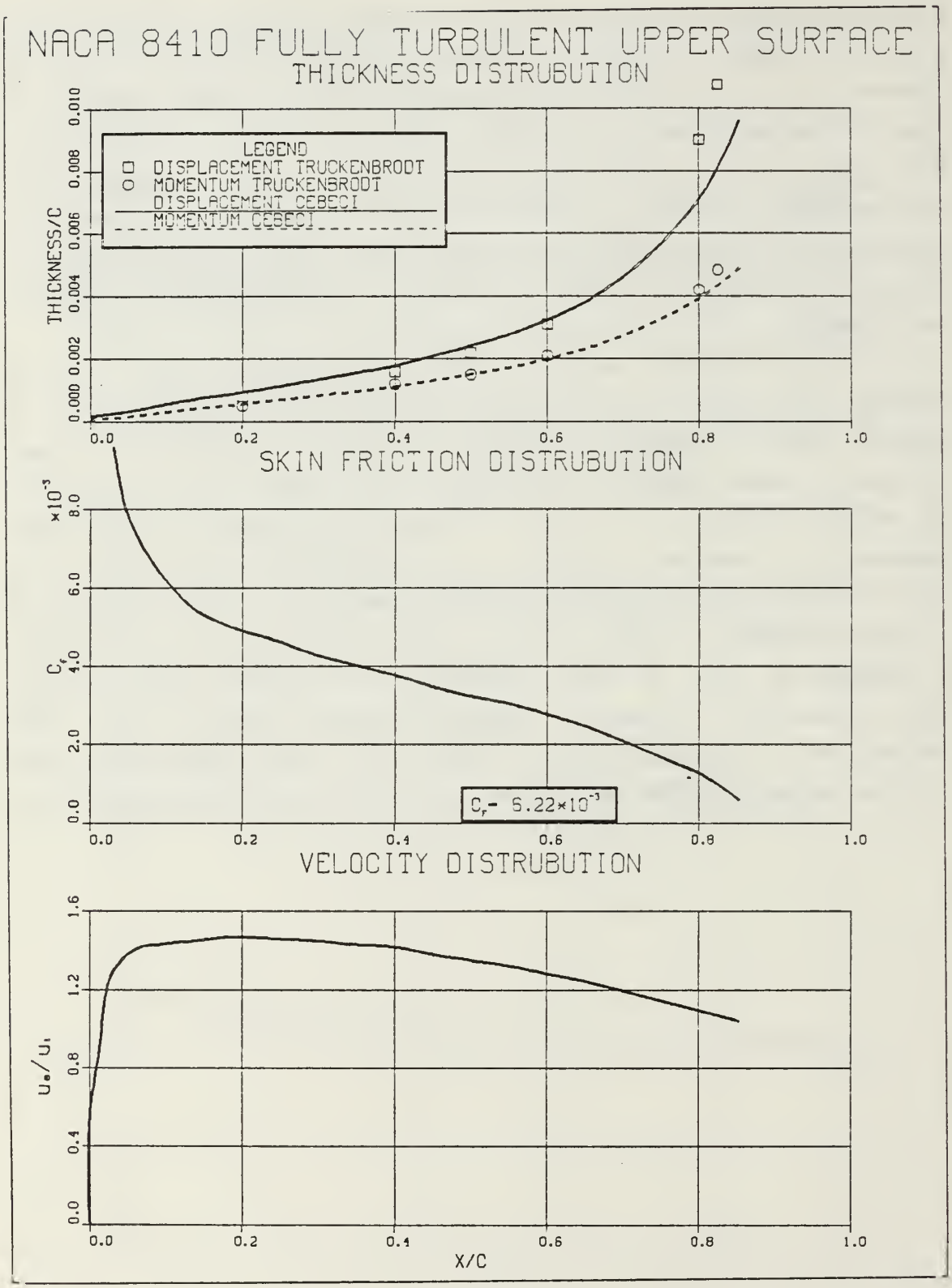

Figure 5.6 NACA 8410 Boundary Layer Results (Suction Side)

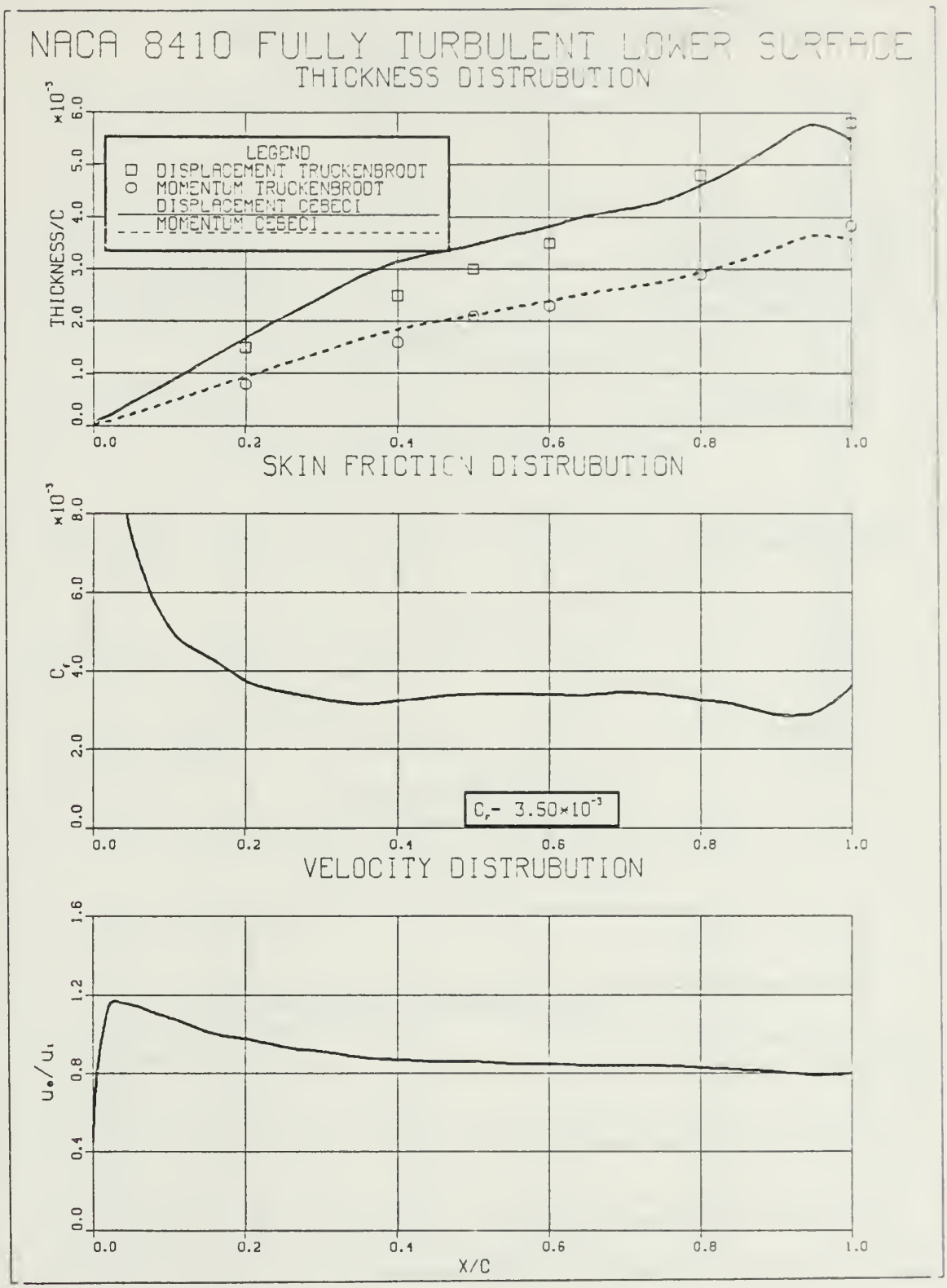

Figure 5.7 NACA 8410 Boundary Layer Results (Pressure Side)

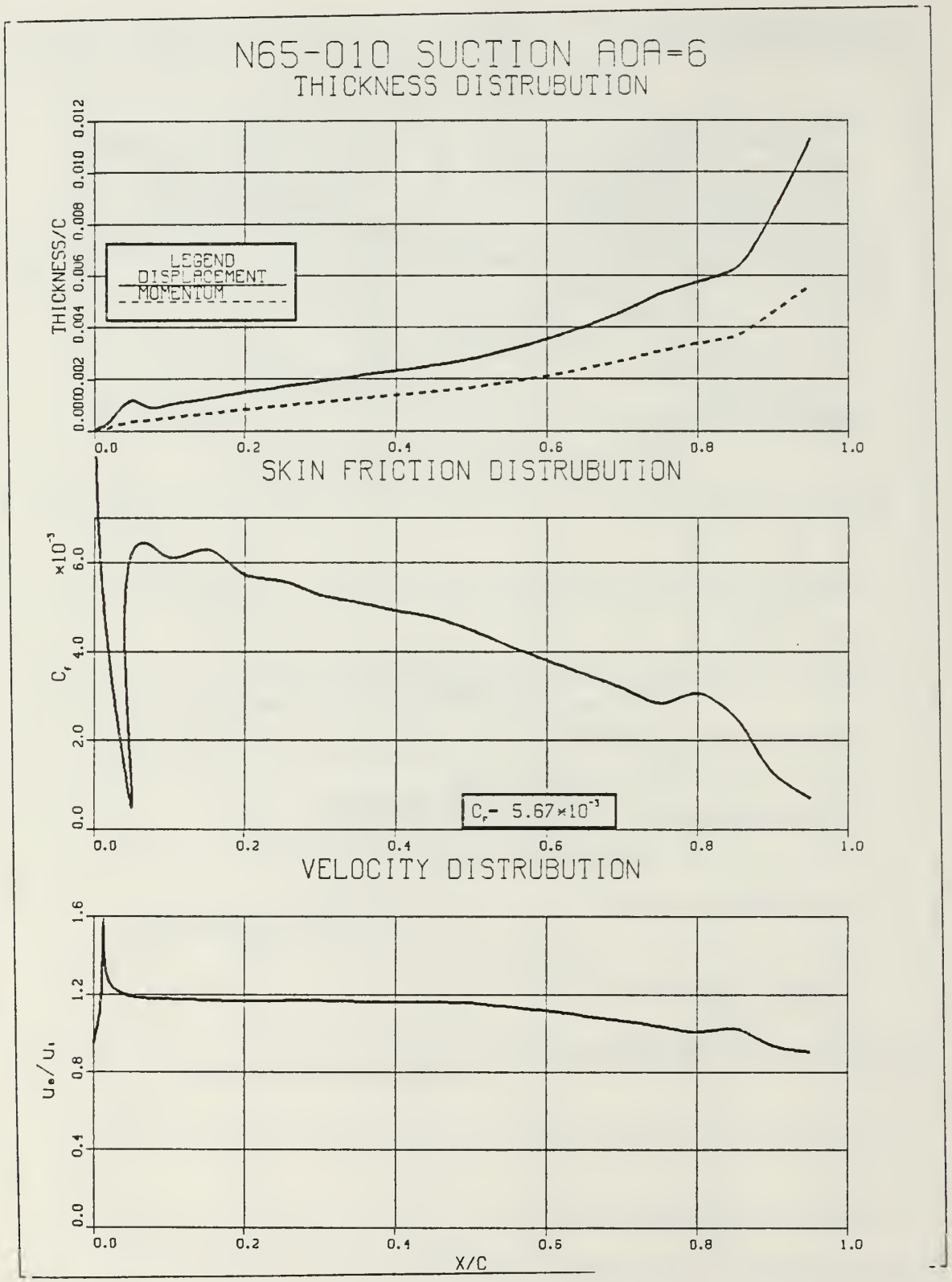

Figure 5.8 NACA 65-010 Boundary Layer Results (Suction Side)

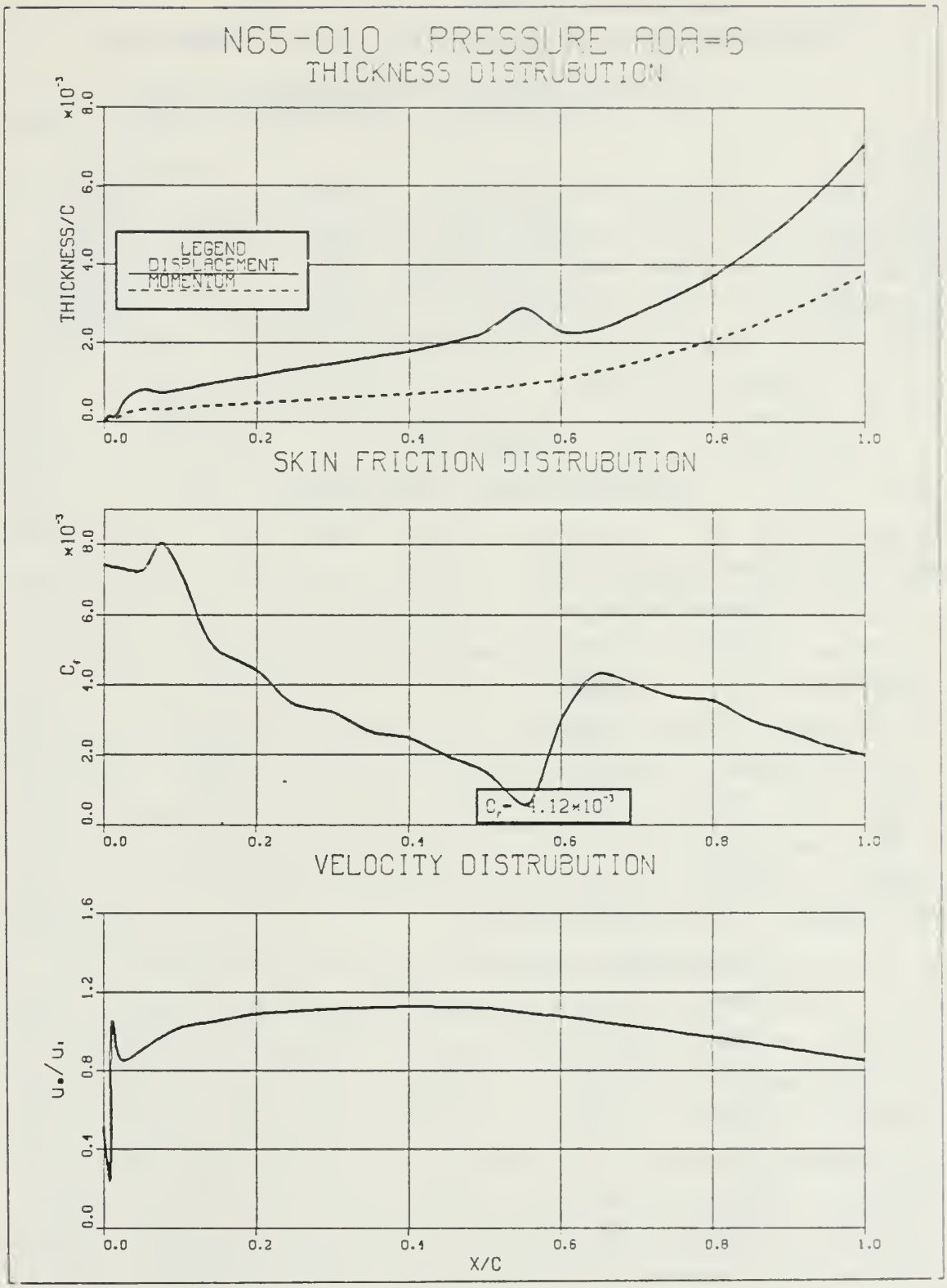

Figure 5.9 NACA 65-010 Boundary Layer Results (Pressure Side)

TABLE II

Comparison of Calculated and Measured Drag Coefficients

AIRFOIL	α	REYNOLDS	PROFILE DRAG EXPERIMENT	PROFILE DRAG CALCULATED
NACA 0012	0°	6 MILLION	.00600	.00562
NACA 0009	0°	6 MILLION	.00575	.00614
NACA 0006	0°	6 MILLION	.00510	.00610
NACA 4412	0°	3 MILLION	.00584	.00693

TABLE III

Separation Points from CEBCAS

NACA 65-010 (Inlet β=30° σ=1.5)

	Approximate x/c	
α	Upper	Lower
-3°	.7	.025
2°	.65	.025
4°	.65	.025
6°	NO	NO
9°	.05	.6
15°	.025	.65

NACA 65(4A I)10 (Inlet β=30° σ=1.)

	Approximate x/c	
α	Upper	Lower
-2.4°	.85	NO
3.4°	NO	.01
5.4°	NO	.01
8.4°	NO	.6
11.4°	NO	NO
17.4°	.025	.65

VI. DISCUSSION/CONCLUSIONS

A. DISCUSSION

The experimental pressure coefficients as found by the program Q3DFLOW agreed well with experimental data when using the Kutta condition or inputting the experimental outlet β with the exception of the fan blade. Q3DFLOW also gave good results when compared with the Schlichting and Gostelow analysis. Disagreement between experiment and Q3DFLOW for the fan blade case may have been due to the fact that the incidence angle run was very close to complete stall (i.e. wind tunnel stall) as evidenced by subsequent runs in the cascade wind tunnel at the slightly higher incidences. The axial velocity/density ratio as measured in the wind tunnel was very high in this case and indicates lack of two-dimensionality. Q3DFLOW accounts for this as a blockage factor through the cascade but is only an linear approximation. These two factors may have contributed to the disagreement between the Q3DFLOW results and experimental data as given for the fan blade. Q3DFLOW may give unrealistic pressure coefficients also . One encountered was as high as -34 . The coordinates used to define the leading and trailing edges may have been the cause since a judicial choice of the coordinates generally alleviated the unrealistic pressure coefficients.

The discontinuous pressure coefficient distribution at the trailing edge on NACA 65-$(4A_2|_{8b})$10 (Figures 4.3 and 4.4) is probably due to the discontinuous geometry at the trailing edge that was input to Q3DFLOW as a "last ditch maneuver" to generate an acceptable finite mesh. Initial attempts to generate an acceptable finite element mesh using coordinates where the trailing edge was sufficiently defined were unsuccessful. (Figure 6.1, coordinates were obtained by blending in the forward 95 % of blade with a 1 % chord radius trailing edge located as given in NACA TN 3817.) NACA TN 3817 indicates that the NACA

65-($4A_2 I_{8b}$)10 may have possibly separated on the concave surface (pressure side) at α's of 3.4° and 5.4° for inlet β = 30° and σ = 1. Figures 4.3 and 4.4 did not show any significant difference between measured and calculated pressure coefficients.

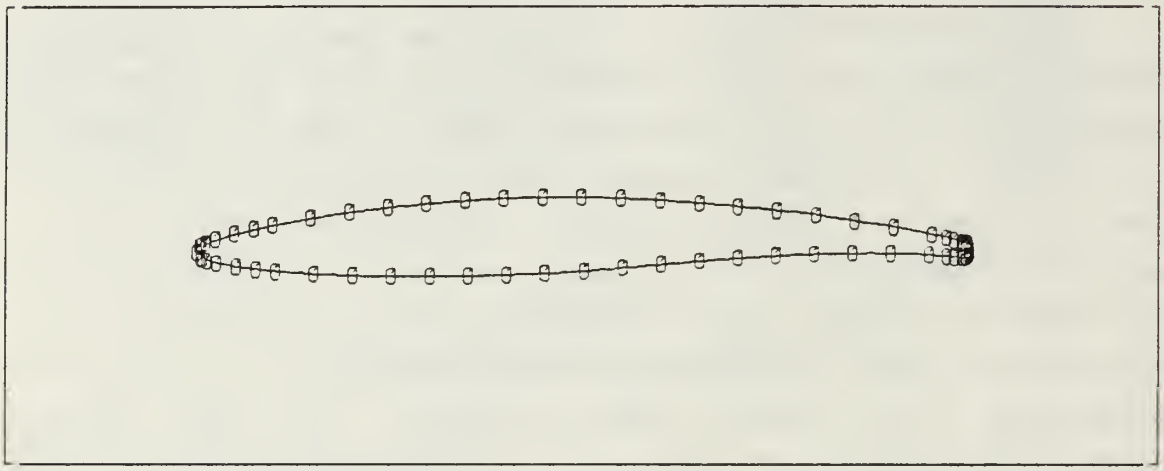

Figure 6.1 NACA 65-($4A_2 I_{8b}$)10 Shape (with Round Trailing Edge Defined)

Experimental data on boundary layers in cascades is sparse at best which makes it difficult to evaluate the merits of the Cebeci boundary layer program. A further difficulty is that most cases run on the Cebeci boundary layer program using Q3DFLOW inviscid incompressible pressure distribution as input indicated separation. High pressure gradients and low Reynold numbers on the leading edge may make the boundary layer equations not valid. However, the calculated drag coefficient for the one case that had a sharp trailing edge and had attached flow on both sides, the NACA 65-010 at α = 6°, did agree well with the measured value.

B. CONCLUSION

Results of the program Q3DFLOW indicate that reasonably correct pressure distributions may be calculated when inputting the leading edge and trailing edge coordinates of a practical compressor blade with

care. The usefulness of the Cebeci program in calculating boundary layers in cascades still remains a question. Use of these two programs in conjunction with each other will probably not give accurate aerodynamic parameters such as lift and drag on practical turbomachinery blades in general due to separation being calculated by the Cebeci boundary layer program.

APPENDIX A
OPERATION OF CEBECI BOUNDARY LAYER PROGRAM

The boundary layer program as sent from Cebeci in September, 1984 calculates total skin friction drag, total profile drag using Squire-Young formula, and transition based on an empirical formula given by Cebeci and Smith [Ref. 10] in addition to those parameters presented in Cebeci and Bradshaw [Ref. 3]. Additionally, the inputs have been modified. The current version of this program used for this thesis has been slightly modified again to give graphical output and to handle numerous data files at once. Another slight modification can calculate losses for cascades using an equation 44 of Reference 15.

A. INPUTS

All inputs are formatted by fortran format. A card will refer to an input line that is a maximum of 80 columns. Each card will be defined by columns, format, variable and explanatory comment. For example:

col 1-5	I5	variable	explanatory commentary

col 1-5	indicates the field assigned to hold the value of the variable
I5	indicates the format used
variable	indicates a fortran name for the variable
explanatory comment	gives information on the variables

Integer format statements are right justified that is in the preceding example if you want the variable to have a integer value of 1 you would put 1 in column 5. If you put the 1 in column 3 the value would be

read as the integer 100. The other two fortran format statements used in this program are F10.0 and 20A4. The F10.0 refers to a floating-point variable. A real number must be specified within the ten position field using a decimal point to separate the decimal point from the mantissa. Any amount of numbers right of the decimal point may be specified as input as long as it fits in the field. The 20A4 refers to a Hollerith variable. 80 positions are available for 80 characters. This format is used to read in the title for the output and the disspla routine (graphics). The last two character of the title must be $' so the disspla routine may read your title. 80 characters are available to specify the title but twenty to thirty are only recommended for the current character height used in the program. This may easily be modified for those familiar with DISSPLA (a graphics software package).

1. *Inputs for CEBPLT*

The following cards give the format to the modified Cebeci program (CEBPLT) that gives graphical output but does not calculate losses for cascades.

$$

Run card Format(I5)

****

col 1-5 I5 N the number of runs (data files)

$$

Title card Format(20A4)

****

col 1-80 20A4 Title tabular and graphics title; last two characters must be $' and immediately next to last character of actual title, recommend only twenty to thirty characters for current character height setting

$$

General card 1 Format(3I5)

****

```
col 1-5    I5      NXT       total x/c or y/c coordinates;
                                 number of x/c coordinates must equal
                                  number of y/c coordinates (i.e.
                                  they are paired)
col 6-10   I5      ITFS      transition flag setter;
                                 set equal to 1 transition calculated
                                  by Michel's method which is given
                                  by Eq.(6.1.1) in Ref. 2 set equal
                                  to 0, transition is input XCTR
                                  (General Card 2 col 41-50)
col 11-15  I5      BC        boundary conditions format;
                                 Set equal to 1 when inputting
                                  velocity ratios, UE, on General card
                                  2, col 31-40 , set to any integer
                                  value other than 1 when inputting
                                  the Coefficient of Pressure ,Cp,
                                  instead of UE
$$$$$$$$$$$$$$$$$$$$$$$$$$$$$$$$$$$$$$$$$$$$$$$$$$$$$$$$$$$$$$$$$$$$$$$$
General card 2               Format(6F10.0)
**********
col 1-10   F10.0   P2(1)     Pressure gradient parameter;
                                 value of m at stagnation point, set
                                  equal to 1.0
col 11-20  F10.0   DETA(1)   initial normal step size,h;
                                 (i.e. is in the neta direction), 0.01
                                  is a good value
col 21-30  F10.0   VGP       Variable grid parameter,k;
                                 defines the ratio of successive step
                                  sizes in the neta direction , 1.14 is
                                  a good value,the higher the value
                                  the fewer calculations performed in
                                  the neta direction
Col 31-40  F10.0   RC        Reynolds number of chord.
Col 41-50  F10.0   XCTR      transition input;
```

x/c coordinate of transition from laminar to turbulent, required if ITFS is 0 (General card 1,Col 6-10)

$$$

Data card 2 Format(3F10.0)

****

col 1-10 F10.0 XC x/c coordinate;
starts at stagnation point, or leading edge,must be in increasing size

col 11-20 F10.0 YC y/c coordinate;
must correspond to the x/c coordinate

col 21-30 F10.0 UE Velocity ratio;
that is the velocity at edge of boundary layer divided by velocity at infinity, must correspond with location (x/c,y/c) and with BC assigned a value 1 (General card 1, col 11-15), Coefficient of Pressure may be inputted instead if BC is a value other than 1

2. *Inputs for CEBCAS*

Inputs to CEBCAS are essentially the same as CEBPLT except for the run card. The run card is modified as follows to input other parameters needed to calculate losses and drag coefficients for cascades.

$$$

Run card Format(I10,3(F10.0))

****

col 1-10 I5 N the number of runs (data files)

col 11-20 F10.0 BTA1 the inlet β (degrees)

col 21-30 F10.0 BTA2 the outlet β (degrees)

col 31-40 F10.0 SIGMA σ

B. OPERATION OF CEBPLT AND CEBCAS

First you must obtain the appropriate fortran program. Link to the AERO disk and send appropriate program to your disk. After you got a copy of CEBPLT or CEBCAS on your disk you must compile the fortran program(s) on an appropriate fortran compiler. FILEDEF's (file definitions) must be defined for data input and for tabular output. An input data file must be created as defined. Execute DISSPLA at a TEK618 graphics terminal for graphics output. For specific details see appropriate computer manuals at the Winston Churchill Computer Center.

APPENDIX B

NACA 65-010 (SHAPE AND COORDINATES)

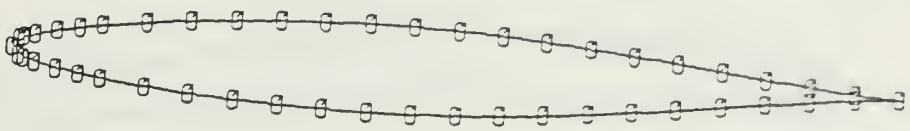

BLADE GEOMETRY IN LOCAL COORDINATE SYSTEM				
FT	UPPER SURFACE		LOWER SURFACE	
	X/C	Y/C	X/C	Y/C
1	0.0	0.0	0.0	0.0
2	0.0075	0.0093	0.0075	-0.0093
3	0.0125	0.0117	0.0125	-0.0117
4	0.0250	0.0157	0.0250	-0.0157
5	0.0500	0.0218	0.0500	-0.0218
6	0.0750	0.0265	0.0750	-0.0265
7	0.1000	0.0304	0.1000	-0.0304
8	0.1500	0.0367	0.1500	-0.0367
9	0.2000	0.0414	0.2000	-0.0414
10	0.2500	0.0450	0.2500	-0.0450
11	0.3000	0.0476	0.3000	-0.0476
12	0.3500	0.0492	0.3500	-0.0492
13	0.4000	0.0500	0.4000	-0.0500
14	0.4500	0.0496	0.4500	-0.0496
15	0.5000	0.0481	0.5000	-0.0481
16	0.5500	0.0453	0.5500	-0.0453
17	0.6000	0.0415	0.6000	-0.0415
18	0.6500	0.0368	0.6500	-0.0368
19	0.7000	0.0316	0.7000	-0.0316
20	0.7500	0.0258	0.7500	-0.0258
21	0.8000	0.0199	0.8000	-0.0199
22	0.8500	0.0138	0.8500	-0.0138
23	0.9000	0.0081	0.9000	-0.0081
24	0.9500	0.0031	0.9500	-0.0031
25	1.0000	0.0	1.0000	0.0

APPENDIX C

NACA 65-(4A I)10 (SHAPE AND COORDINATES)

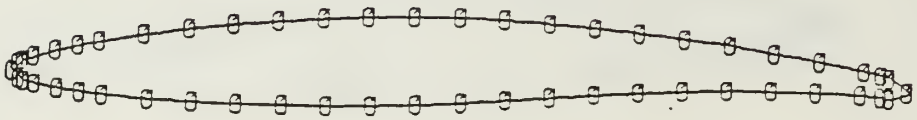

BLADE GEOMETRY IN LOCAL COORDINATE SYSTEM				
PT	UPPER SURFACE		LOWER SURFACE	
	X/C	Y/C	X/C	Y/C
1	0.0	0.0	0.0	0.0
2	0.0069	0.0098	0.0081	-0.0088
3	0.0118	0.0125	0.0132	-0.0109
4	0.0241	0.0172	0.0259	-0.0142
5	0.0488	0.0247	0.0512	-0.0188
6	0.0736	0.0307	0.0764	-0.0221
7	0.0984	0.0360	0.1016	-0.0247
8	0.1481	0.0449	0.1520	-0.0283
9	0.1979	0.0523	0.2021	-0.0304
10	0.2478	0.0585	0.2522	-0.0315
11	0.2978	0.0635	0.3022	-0.0316
12	0.3478	0.0674	0.3522	-0.0310
13	0.3981	0.0702	0.4019	-0.0297
14	0.4483	0.0717	0.4517	-0.0275
15	0.4987	0.0717	0.5013	-0.0245
16	0.5491	0.0701	0.5509	-0.0205
17	0.5995	0.0671	0.6005	-0.0160
18	0.6500	0.0634	0.6500	-0.0117
19	0.7004	0.0591	0.7004	-0.0079
20	0.7508	0.0541	0.7492	-0.0048
21	0.8012	0.0481	0.7988	-0.0026
22	0.8516	0.0400	0.8484	-0.0016
23	0.9017	0.0326	0.8983	-0.0018
24	0.9518	0.0227	0.9482	-0.0037
25	0.9700	0.0187	0.9700	-0.0055
26	0.9800	0.0155	0.9800	-0.0068
27	1.0000	0.0	1.0000	0.0

APPENDIX D

NACA 8410 (SHAPE AND COORDINATES)

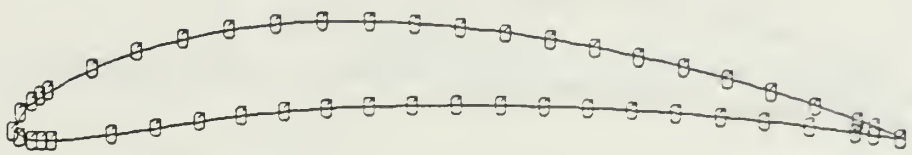

BLADE GEOMETRY IN LOCAL COORDINATE SYSTEM				
PT	UPPER SURFACE		LOWER SURFACE	
	X/C	Y/C	X/C	Y/C
1	0.0	0.0	0.0	0.0
2	0.0088	0.0219	0.0074	-0.0069
3	0.0218	0.0337	0.0212	-0.0102
4	0.0309	0.0405	0.0327	-0.0107
5	0.0402	0.0467	0.0437	-0.0104
6	0.0888	0.0724	0.1112	-0.0024
7	0.1392	0.0920	0.1608	0.0055
8	0.1906	0.1069	0.2094	0.0131
9	0.2427	0.1177	0.2573	0.0198
10	0.2950	0.1248	0.3050	0.0252
11	0.3475	0.1283	0.3525	0.0292
12	0.4000	0.1284	0.4000	0.0316
13	0.4510	0.1259	0.4490	0.0329
14	0.5020	0.1219	0.4980	0.0337
15	0.5527	0.1162	0.5473	0.0338
16	0.6034	0.1090	0.5966	0.0332
17	0.6538	0.1003	0.6462	0.0319
18	0.7040	0.0903	0.6960	0.0297
19	0.7540	0.0788	0.7460	0.0268
20	0.8038	0.0660	0.7962	0.0229
21	0.8534	0.0518	0.8466	0.0182
22	0.9026	0.0362	0.8974	0.0127
23	0.9516	0.0193	0.9484	0.0062
24	0.9711	0.0122	0.9689	0.0034
25	1.0000	0.0	1.0000	0.0

APPENDIX E

CUSPED BLADE (SHAPE AND COORDINATES)

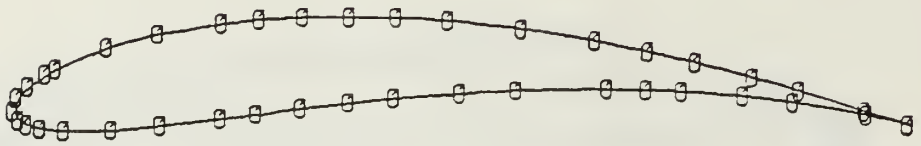

BLADE GEOMETRY IN LOCAL COORDINATE SYSTEM

PT	UPPER SURFACE		LOWER SURFACE	
	X/C	Y/C	X/C	Y/C
1	0.0	0.0	0.0	0.0
2	0.0046	0.0153	0.0060	-0.0099
3	0.0170	0.0288	0.0152	-0.0151
4	0.0356	0.0423	0.0309	-0.0192
5	0.0469	0.0490	0.0576	-0.0215
6	0.1048	0.0738	0.1110	-0.0194
7	0.1616	0.0901	0.1654	-0.0135
8	0.2322	0.1032	0.2320	-0.0046
9	0.2746	0.1082	0.2725	0.0010
10	0.3232	0.1117	0.3220	0.0078
11	0.3750	0.1120	0.3750	0.0150
12	0.4273	0.1124	0.4251	0.0203
13	0.4848	0.1094	0.4999	0.0274
14	0.5685	0.1010	0.5623	0.0317
15	0.6501	0.0889	0.6649	0.0350
16	0.7105	0.0776	0.7085	0.0348
17	0.7630	0.0662	0.7481	0.0337
18	0.8266	0.0505	0.8168	0.0295
19	0.8792	0.0362	0.8731	0.0236
20	0.9520	0.0146	0.9538	0.0107
21	1.0000	0.0	1.0000	0.0

APPENDIX F

FAN BLADE (SHAPE)

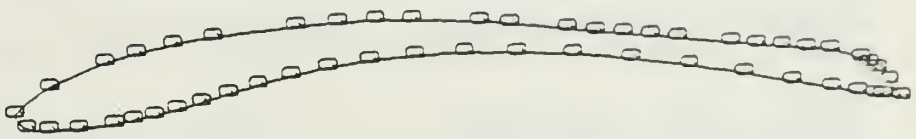

LIST OF REFERENCES

1. Karamcheti K., *Principles of Ideal-Fluid Aerodynamics*, Wiley, New York, 1966.

2. Schlichting H. , *Boundary-Layer Theory*, McGraw-Hill Book Company, New York, 1968.

3. Cebeci T. and Bradshaw P., *Momentum Transfer in Boundary Layers*, Hemisphere Publishing Corporation, Washington, 1977.

4. Hirsch Ch. and Warzee G., "A Finite Element Method for Through-flow Calculations in Turbomachines", Transactions of the ASME, *Journal of Fluids Engineering*, v. 98, pp. 403-422, 1976.

5. Hirsch Ch. and Warzee G., "An Integral Quasi 3-D Finite Element Calculation Program for Turbomachinery Flows", ASME, *Journal of Engineering for Power*, v. 101, pp. 141-148, Jan 1979.

6. Gostelow J. P., *Cascade Aerodynamics*, Pergamon Press, 1984.

7. Miller M. J., Serovy G. K., "Deviation Angle Estimation for Axial-Flow Compressors Using Inviscid Flow Solutions", *Journal of Engineering for Power*, April, 1975.

8. Gostelow J. P., *Trailing-Edge Flows Over Turbomachine Blades and the Kutta-Joukowsky Condition*, ASME-Paper 75-GT-94, 1975.

9. Author unknown, *Computer Program for Turbomachinery Flows/Finite Element Method/User's Guide*, 11 May 1983.

10. Cebeci, T. and A. M. O. Smith, *Analysis of Turbulent Boundary Layers*, Academic Press, New York, 1974.

11. Cebeci T., Keller H. B., "Accurate Numerical Method for Boundary-Layer Flows II: Two-Dimensional Turbulent Flows", *AIAA Journal* , Nov. 1972.

12. Emery J. C., Erwin J. R., Herrig L. J., *Systematic Two-Dimensional Cascade Tests of NACA 65-Series Compressor Blades at Low Speeds*, NACA TN 3916 , 1957.

13. Emery J. C., Erwin J. R., Savage M., *Two-Dimensional Low Speed Cascade Investigation of NACA Compressor Blade Sections having a Systematic Variation in Mean-Line Loading*, NACA TN 3817, 1956.

14. Scholz N., translated and revised by Klein A. from the original German *Aerodynamik der Shaufelgitter*, AGARD-AG-220, 1977.

15. Roudebush W. H., Lieblein S., *Theoretical Loss Relations for Low Speed Two-Dimensional Cascade Flow*, NACA TN 3662, 1956.

16. Abbott I. H. and von Doenhoff A. E. , *Theory of Wing Sections*, Dover, New York, 1959.

17. Pinkerton R. , *Pressure Distributions over the Mid-span Section of the NACA 4412 Airfoil*, NACA Rept. 563, 1936.

INITIAL DISTRIBUTION LIST

No.		Copies
1.	Defense Technical Information Center Cameron Station Alexandria, Virginia 22314	2
2.	Library, Code 0142 Naval Postgraduate School Monterey, California 93943	2
3.	Chairman, Dept. of Aeronautics Code 67 Naval Postgraduate School Monterey, California 93943	10
4.	Professor O. Biblarz Code 67Bi Naval Postgraduate School Monterey, California 93943	1
5.	Commanding Officer Attn: Captain P. E. Genskow Naval Aviation Rework Facility Marine Corps Air Station Cherry Point, North Carolina 28533	3

Thesis
G25977 Genskow
c.1 Analysis of incompressible cascade flows using "state-of-the-art" computer programs.